Nanophysics with local probes
Part I

Hervé Courtois

Institut Néel
CNRS, Université Grenoble Alpes and Grenoble INP

Part II: will be given by H. Sellier

Hervé Courtois

- Professor at Université Grenoble Alpes
- Teacher at UFR PhITEM
- Researcher at Institut Néel
  http://neel.cnrs.fr/spip.php?rubrique804
  Research in quantum electronics: superconducting proximity effect, (hybrid) Josephson junctions, thermal transport at nano-scale
  Development of scanning probe microscopes at low temperature

- Honorary member of Institut Universitaire de France
  Associate director (2011-14) and director (2015) of Néel Institute
  Head of Physics, Engineering & Materials Research Department at Univ. Grenoble Alpes (2015-19).
- Contact: herve.courtois@neel.cnrs.fr

Chapter 0
Introduction

Chapter 0
Introduction

0.1: Near field

What is near field?

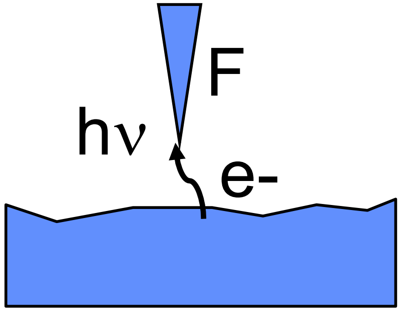

A physical object / field near a sample.

Opposed to far field.

The near-field regime gives access to new physical behaviors.

photons: evanescent light wave
electrons: electron wave-function
forces: VDW forces
…

What is near field microscopy?

Scan a near field probe over a sample.

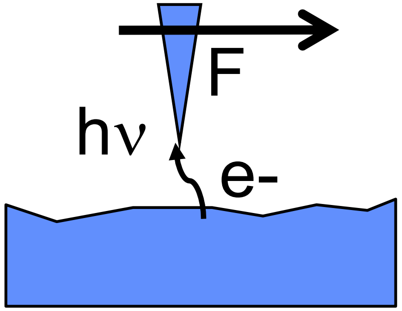

The measured quantity is measured / used for distance regulation.

Near-Field Microscopies also called Scanning Probe Microscopies (SPM) are numerous.

Chapter 0
Introduction

0.2: A gallery

Si (111) 7x7

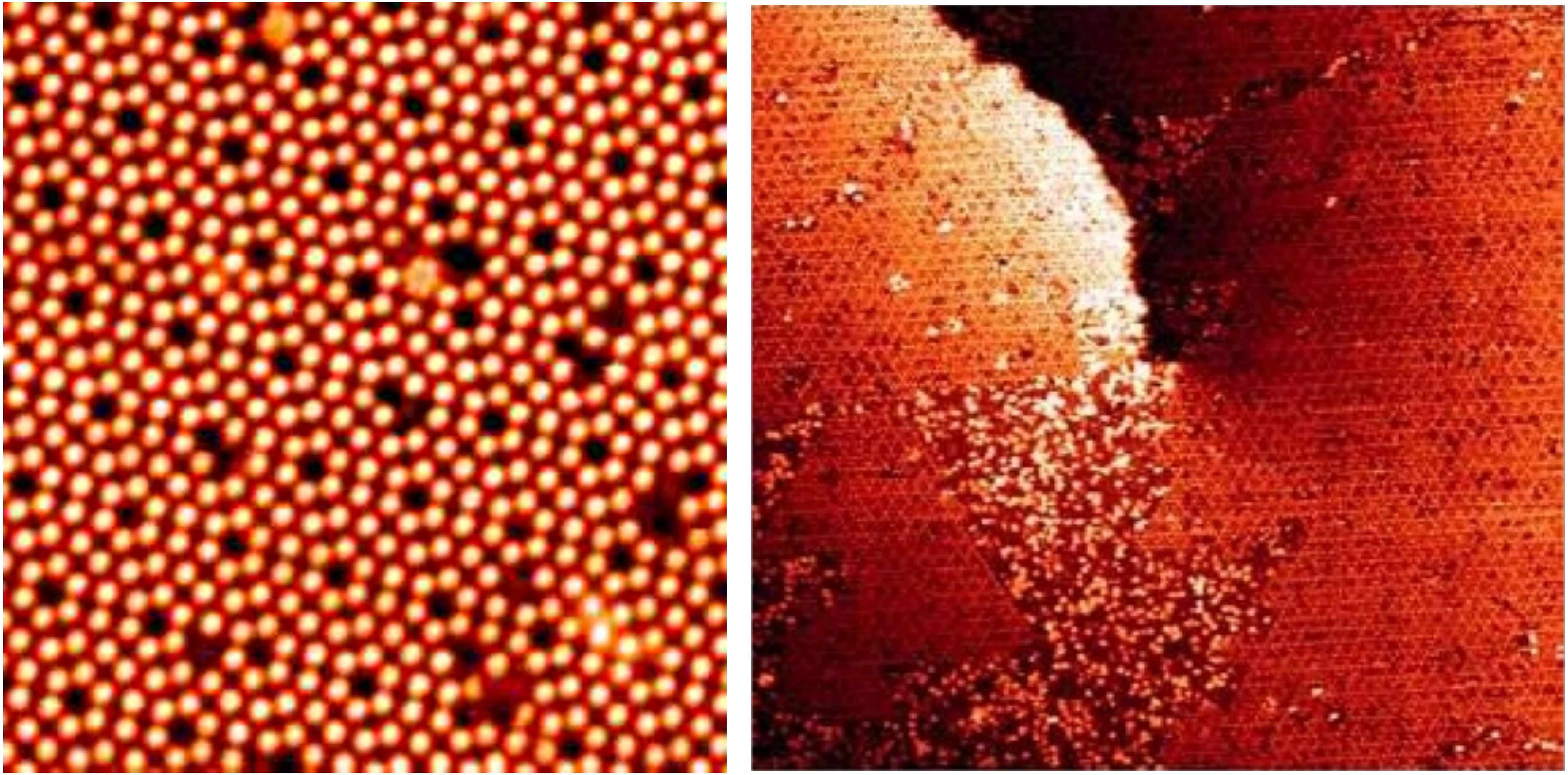

Single vacancies, adsorbates, screw dislocations are visible: true atomic resolution. (Omicron website)

The carbon family

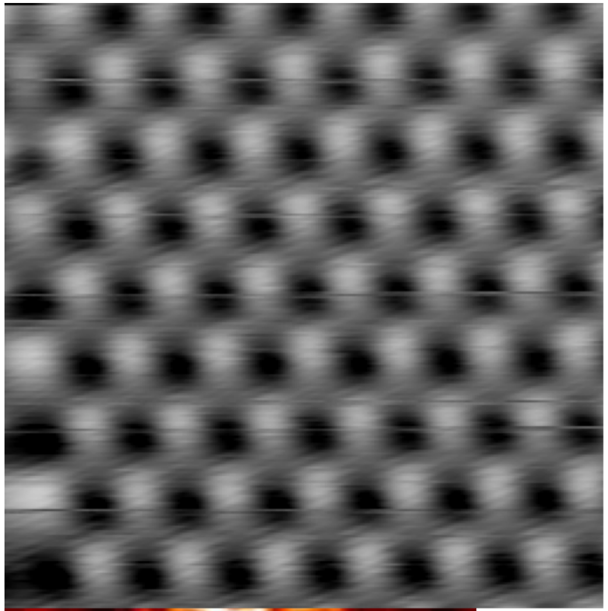

H. Courtois et al; J.W.G. Wildoer et al, Nature 391, 59 (1998)
K. Bibrov et al, Nature 413, 616 (2001) ;
P. Mallet, J.Y. Veuillen et al, Phys. Rev. B 76, 041403(R) (2007).

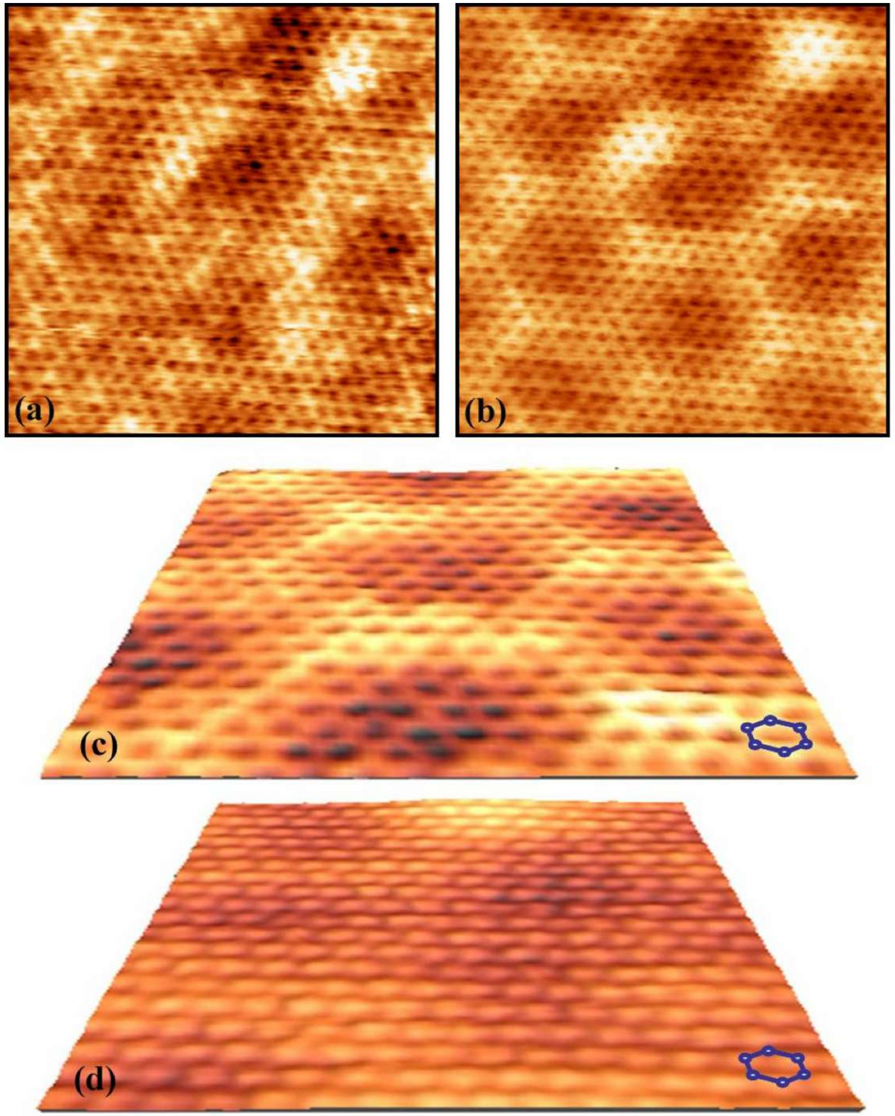

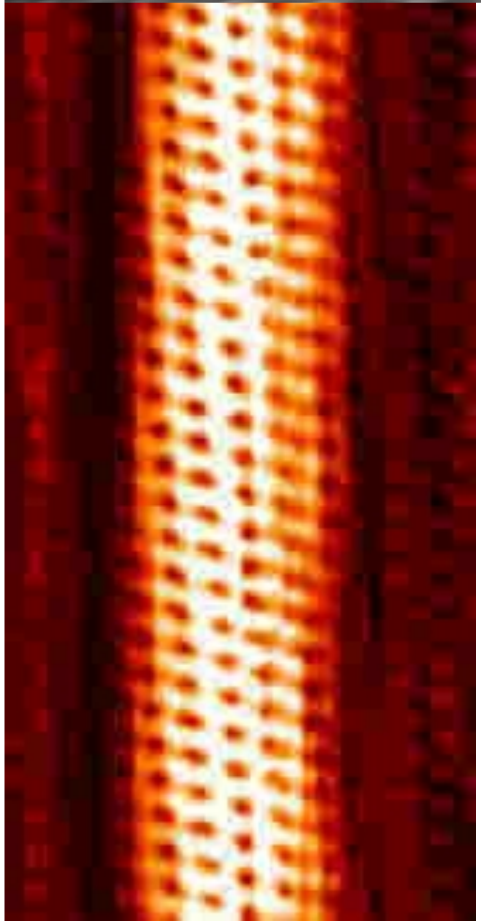

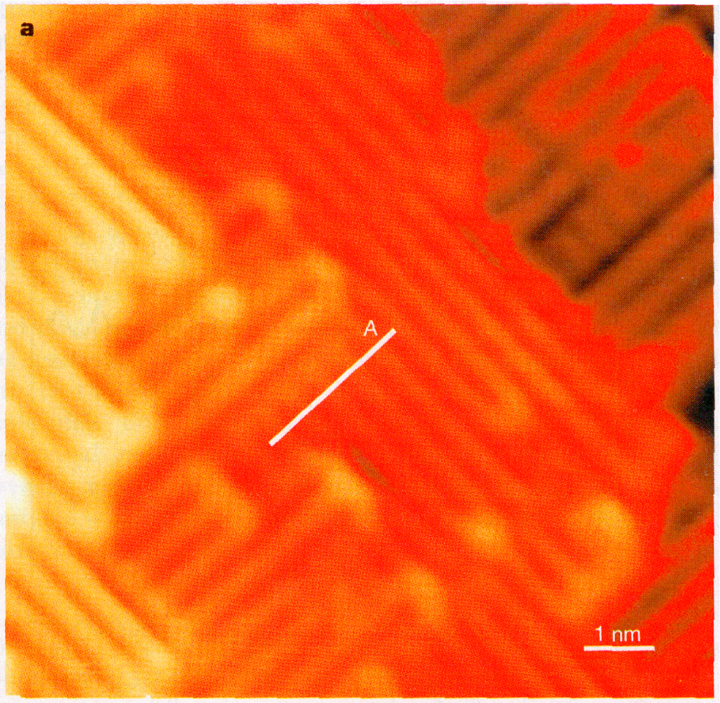

Carbon nanotubes

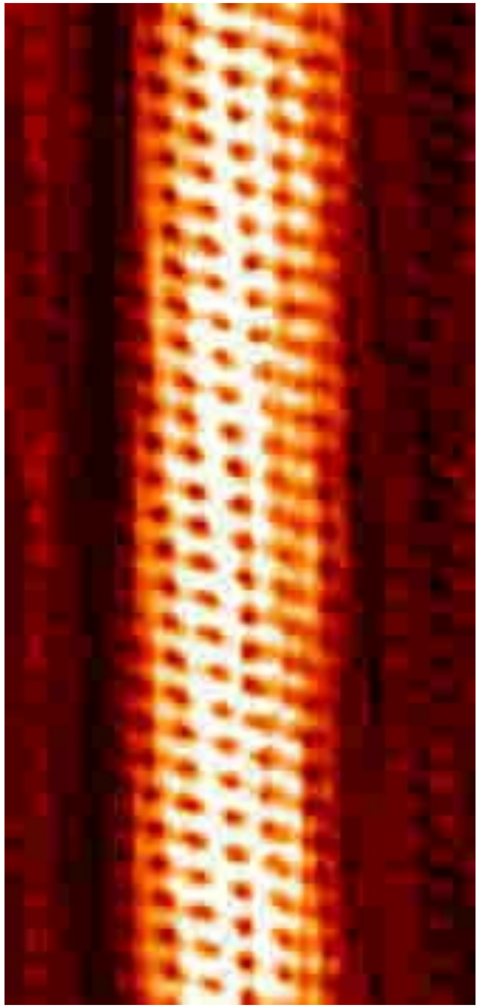

NT on a Au surface.

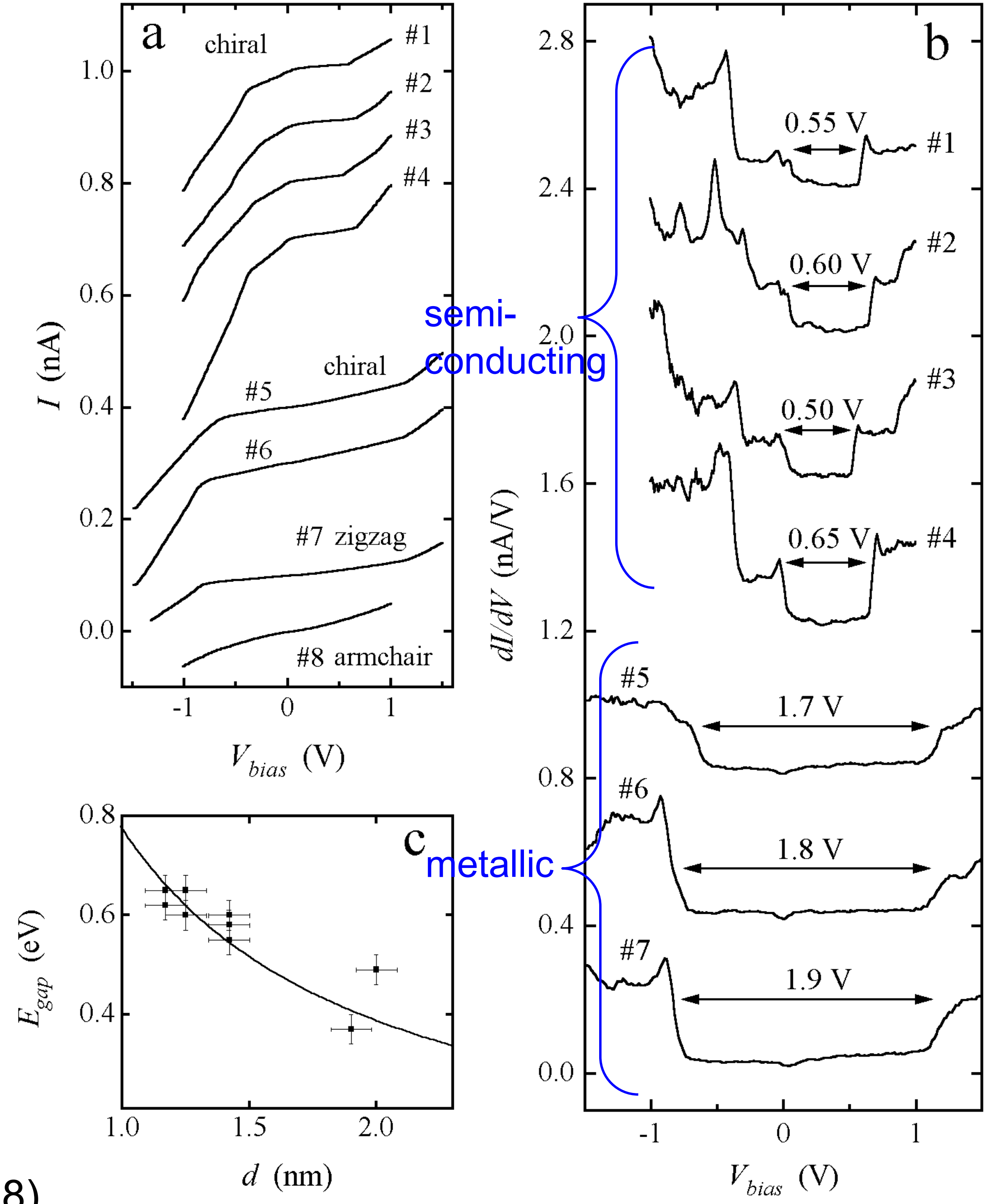

J.W.G. Wildoer et al, Nature 391, 59 (1998)

The chemical contrast

As = red atoms / open circles

Ga = green / closed.

J. Stroscio et al, Phys. Rev. Lett. 58, 1192 (1987).

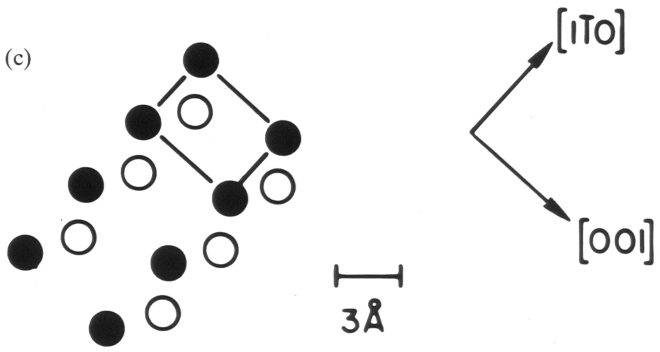

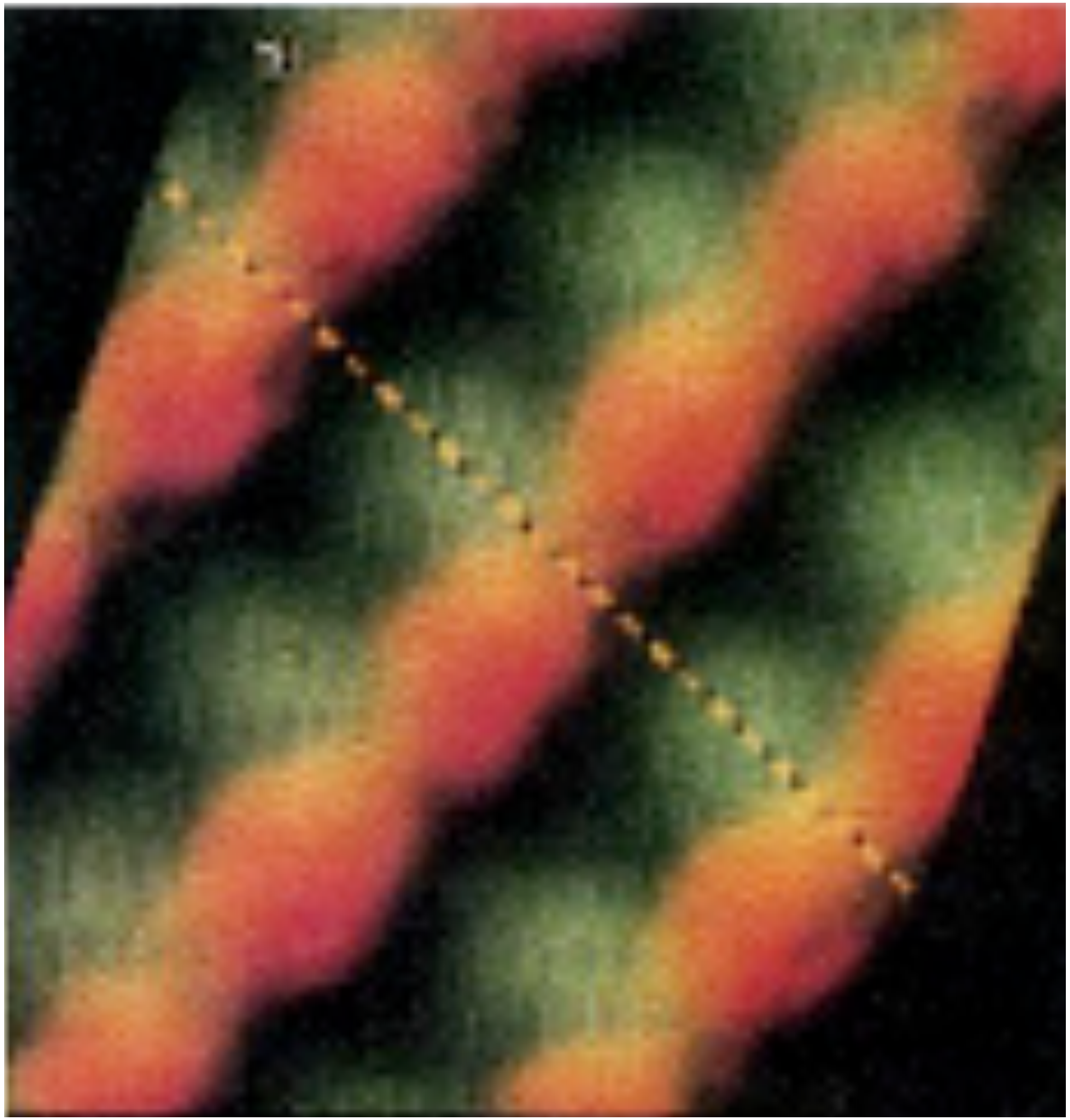

Chemical reactions observation

C. Sachs, M. Hildebrand, S. Völkening, J. Wintterlin and G. Ertl, Science 293, 1635 (2001).

Front moves at about 15 nm/min

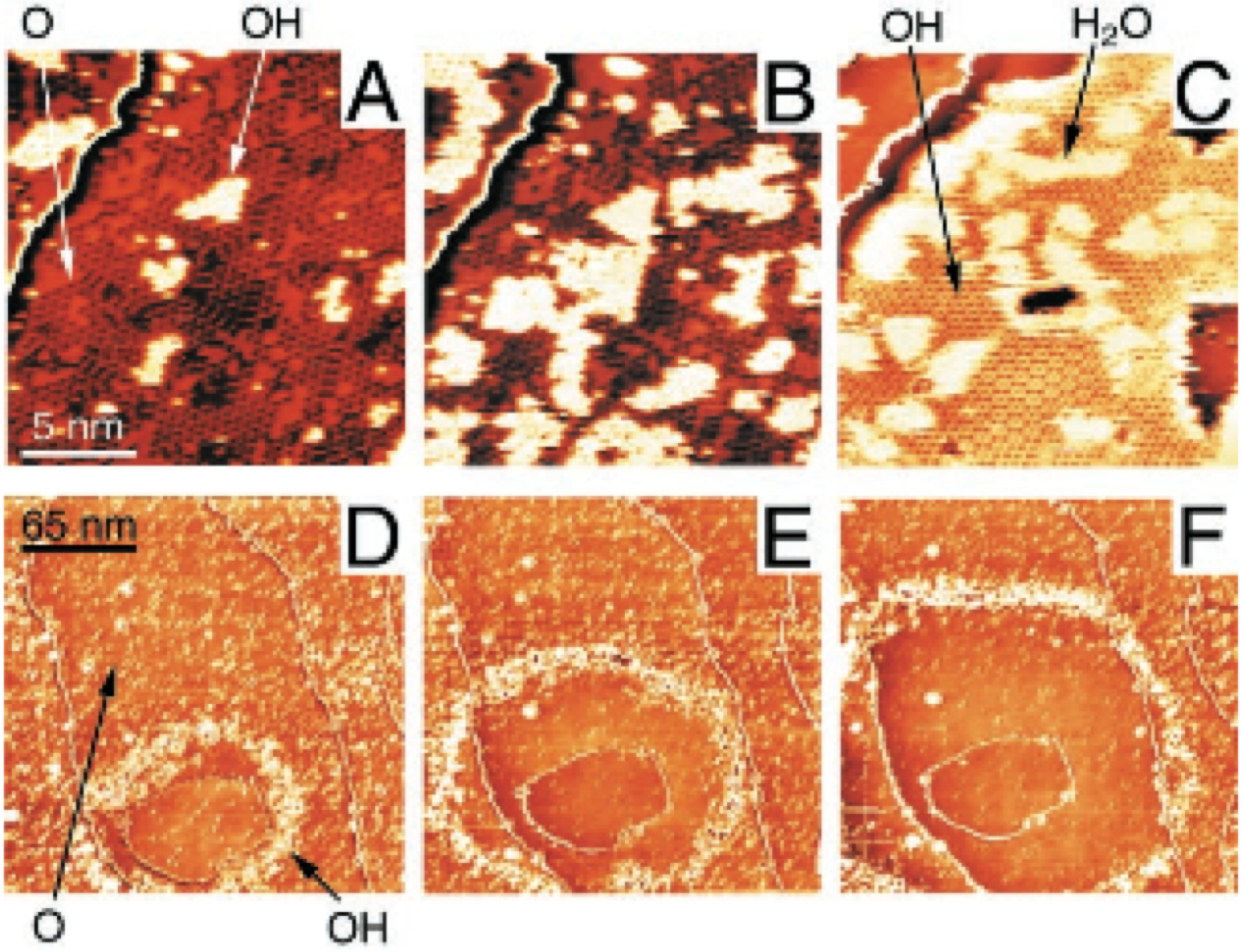

Fig. 1. Series of successive STM images, recorded during dosing of the O-covered Pt(111) surface with H_2. (A to C) Frames (17 nm by 17 nm) from an experiment at 131 K [$P(H_2) = 8 \times 10^{-9}$ mbar]. The hexagonal pattern in (A) is the (2 × 2)O structure; O atoms appear as dark dots and bright features are the initial OH islands. In (C), the area is mostly covered by OH, which forms ordered ($\sqrt{3}\times\sqrt{3}$)R30° and (3×3) structures. The white, fuzzy features are H_2O-covered areas. (D to F) Frames (220 nm by 220 nm) from an experiment at 112 K [$P(H_2) = 2 \times 10^{-8}$ mbar]. In (D), the surface is mostly O-covered (not resolved). The bright dots are small OH islands, most of which are concentrated in the expanding ring. H_2O in the interior of the ring is not resolved here. Thin, mostly vertical lines are atomic steps.

Imaging individual polymers

UHV STM and STS of Poly(3-dodecylthiphene) monolayers (di-block polymer) on HOPG.

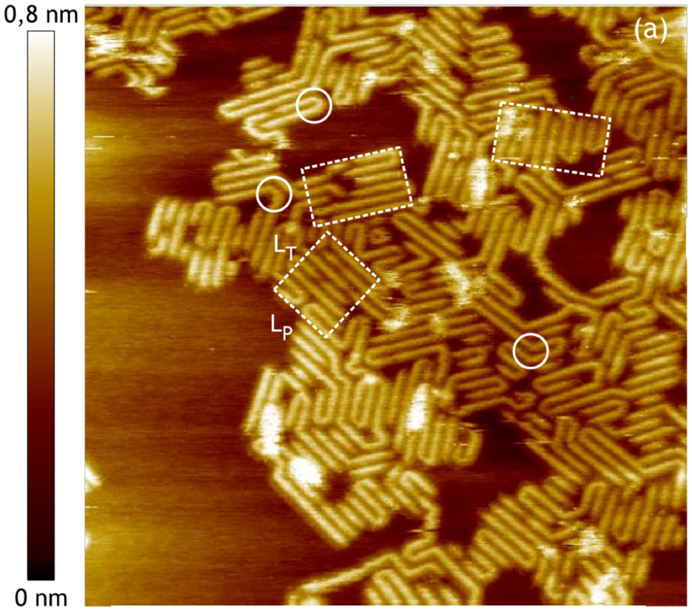

B. Grévin et al, SPRAM, Grenoble : L. Scifo et al, Nano Lett. 6, 1711 (2006).

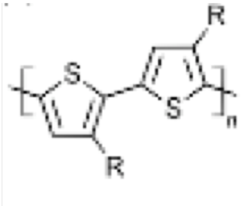

P3DDT : R = $C_{12}H_{25}$

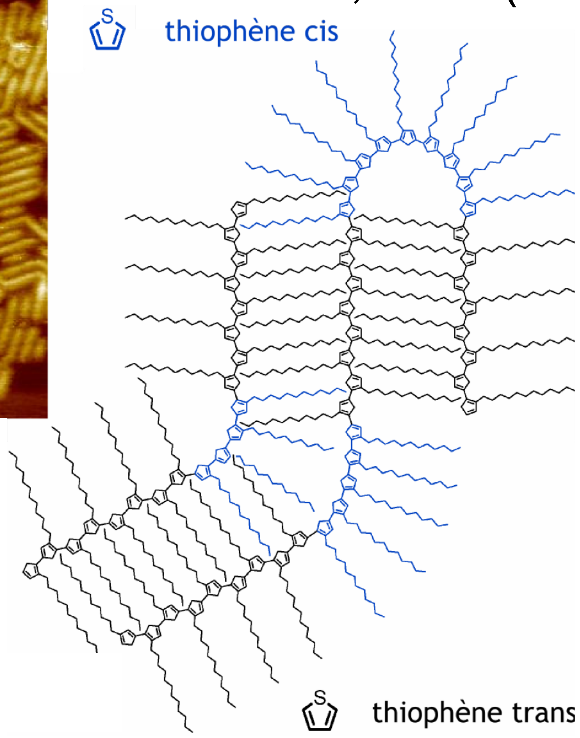

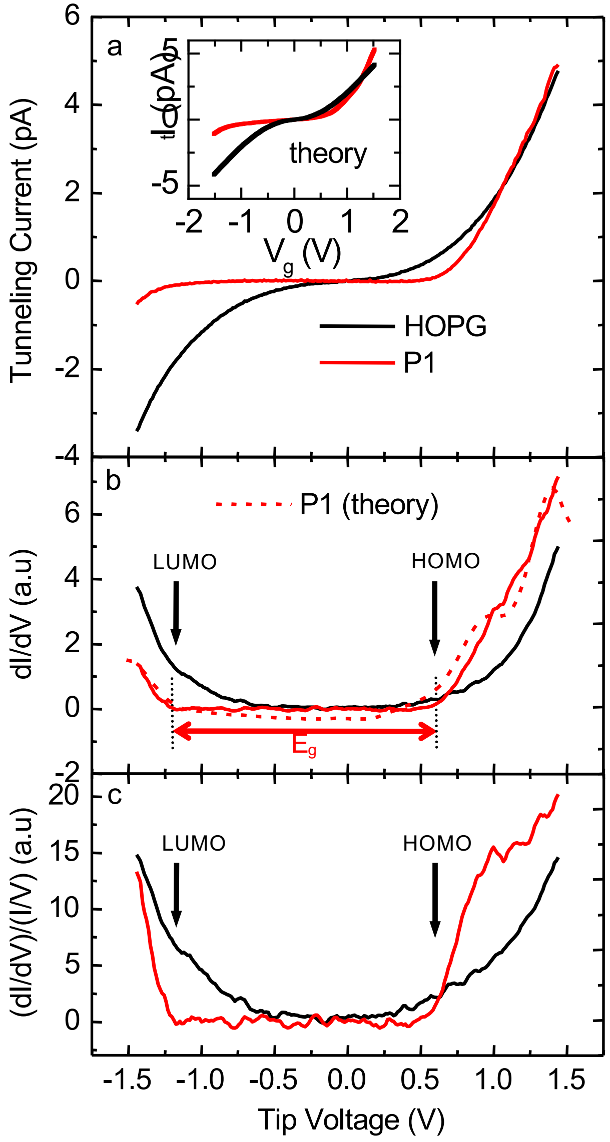

The vortex lattice

A superconductor under magnetic field

H.F. Hess et al., Phys. Rev. Lett. 62, 214 (1989).

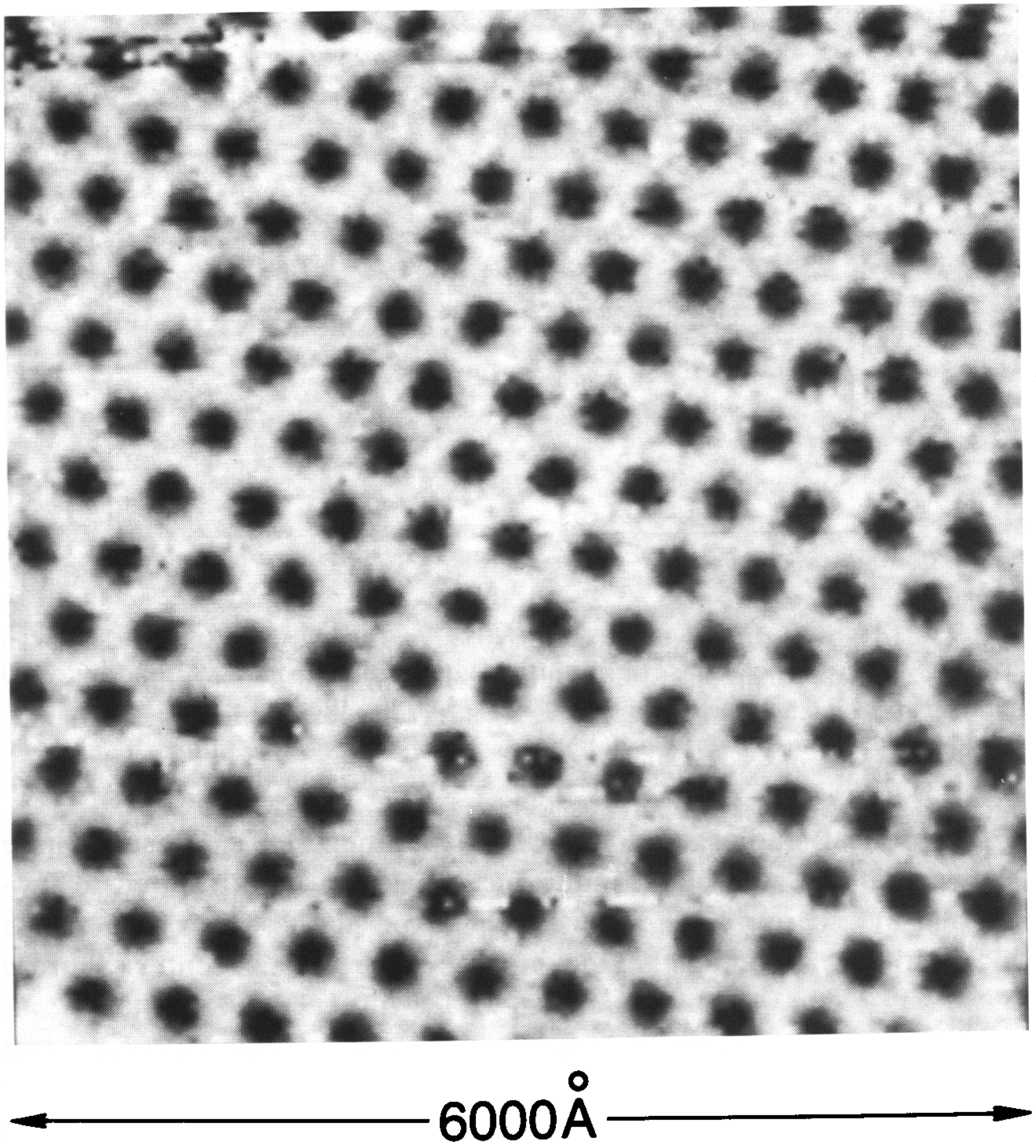

Fig. 4.120. Abrikosov flux lattice produced by 1 T magnetic field in NbSe$_2$ at 1.8 K. The gray scale corresponds to dI/dU (Hess *et al.*, 1989).

Spin-resolved STM

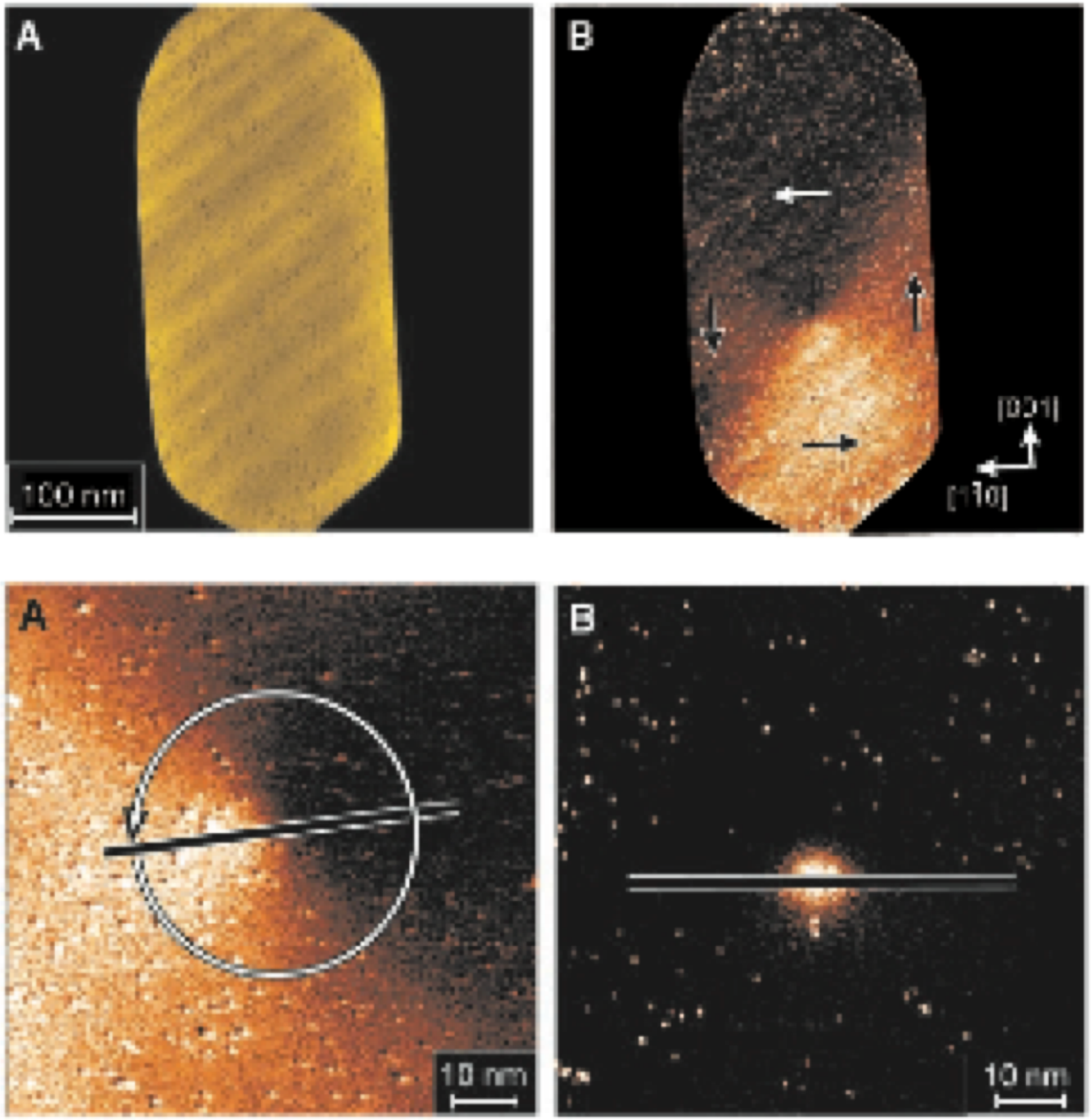

A magnetic vortex.

A. Wachowiak et al, Science 298, 577 (2002).

Quantum corrals

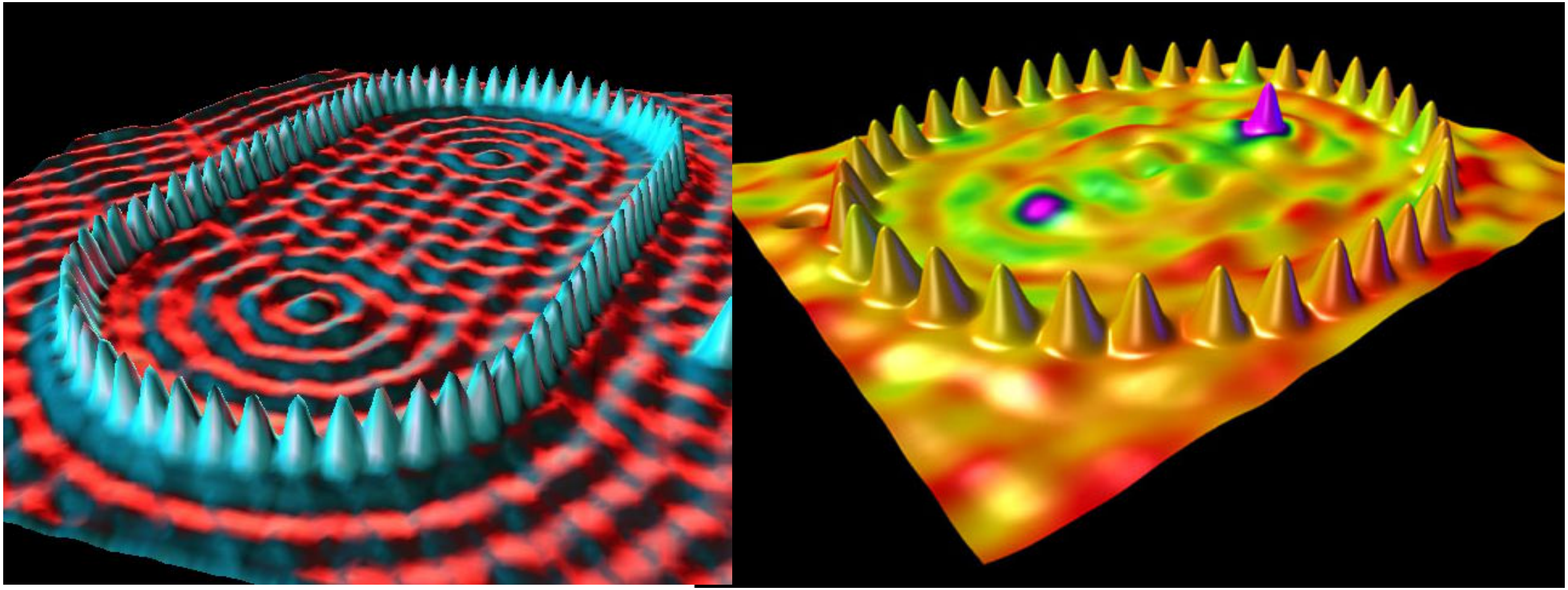

Co atoms on a Cu surface

M.F. Crommie, C.P. Lutz and D.M. Eigler, Science 262, 218 (1993); H.C. Manoharan, C.P. Lutz and D.M. Eigler, Nature 403, 512 (2000).

Chapter 0
Introduction

0.3: About this course

This lecture objectives

Learn the physical principles in STM,

General instrumentation for SPMs,

Review STM applications in various scientific fields.

Outline

Chapter 0: Introduction
Near field, gallery, about, conventional microscopies

Chapter 1: Scanning Tunneling Microscopy
DOS, work-function, square barrier model, tunnel current, history, field emission

Chapter 2: Instrumentation for the STM and AFM
Tips, Piezo-electricity, actuators, displacements, scanning, positioning, design rules, electronics

Chapter 3: STM imaging
Principles, resolution, Si 7x7, imaging at various bias, HOPG, graphene

Chapter 4: STM spectroscopy (STS)
Principles, superconductors, IETS, graphene, nanotubes, spin resolution, Kondo mirage

General references

"Scanning probe microscopy : methods and applications", R. Wiesendanger, Cambridge University Press (1994). A very good reference on many kinds of scanning probes.

"Introduction to scanning tunneling microscopy", C. J. Chen, Oxford series in optical and imaging techniques, Oxford University Press (1993). Best reference for STM intrumentation.

“Les nouvelles microscopies”, L. Aigouy, Y. de Wilde and C. Fretigny, Belin (2006).

“Scanning Probe Microscopy: The Lab on a Tip“, Ernst Meyer, Hans J. Hug, Roland Bennewitz (2004).

General information

Take notes during the lectures !

Do not hesitate to ask questions !

Questions session at the beginning of every lecture.

Slides available as pdf at http://neel.cnrs.fr/spip.php?rubrique804

Oral exam. No documents, no PC.

Chapter 0
Introduction

0.4: Conventional microscopies

Optical microscopy and the Rayleigh criteria

Resolution limited by Fraunhofer diffraction

$$r = k\frac{\lambda}{NA}$$

NA : numerical aperture = n sin(i)

k = 0.61 in theory: Rayleigh criteria

$r \approx \lambda \approx 0.5$ µm in practice

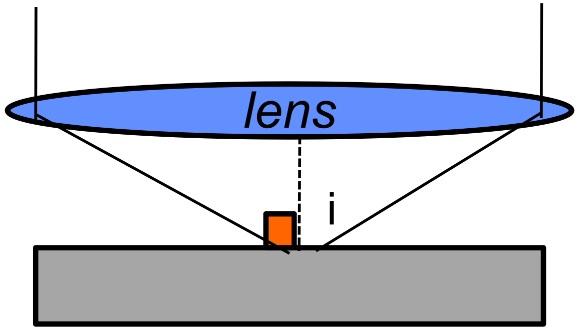

Depth of focus

$$DoF = \frac{\lambda}{2\,NA^2}$$

Scanning Electron Microscopy : SEM

The electron (e^-) beam (2-50 keV) is shaped, focused by magnetic lenses, and scanned.

Secondary (or backscattered) e^- are collected to build an image.

e^- wavelength 10 pm, resolution of about 10 nm limited by beam size and interaction volume.

Charges need to be evacuated: conductive surfaces only. Under vaccuum.

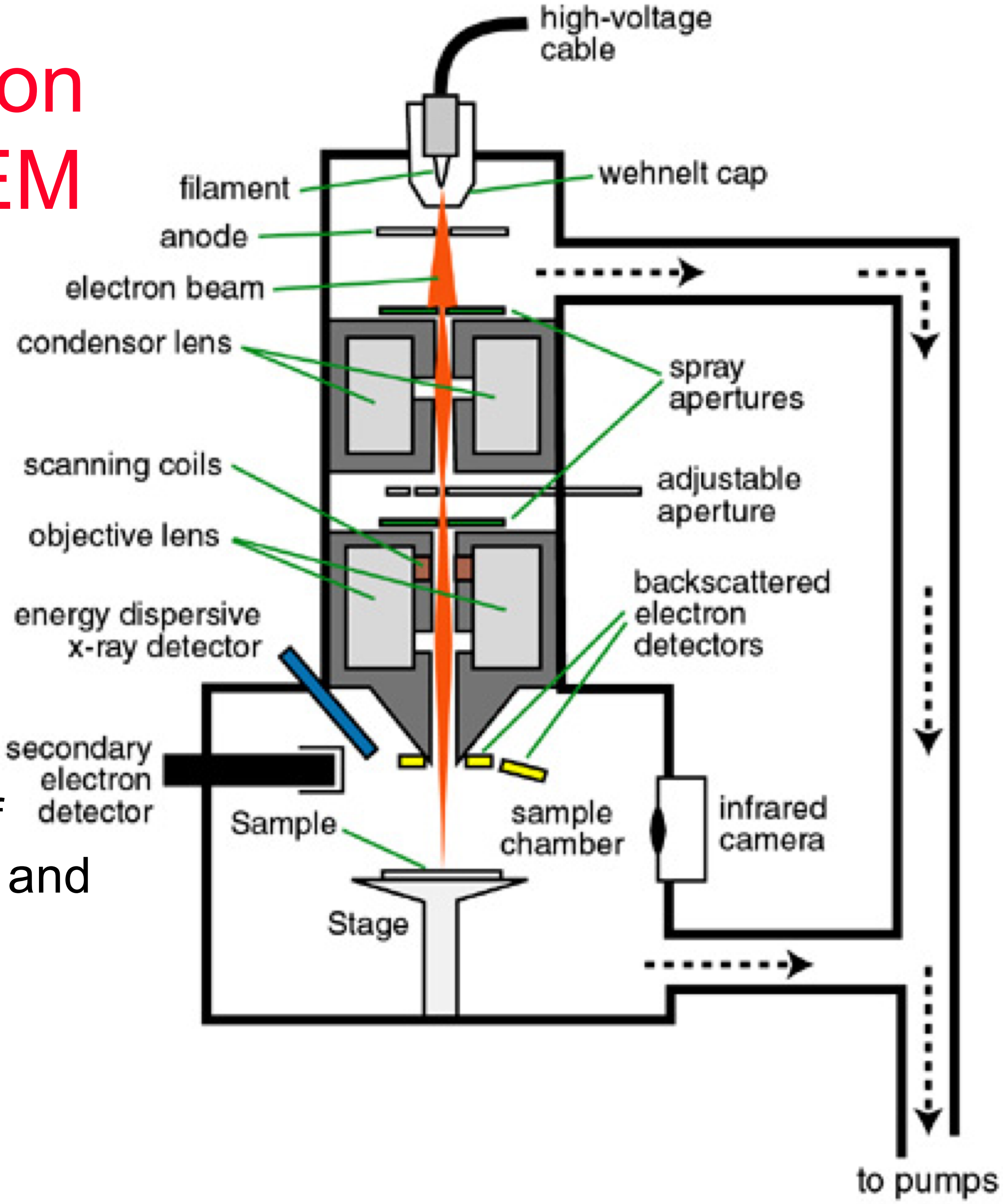

SEM images

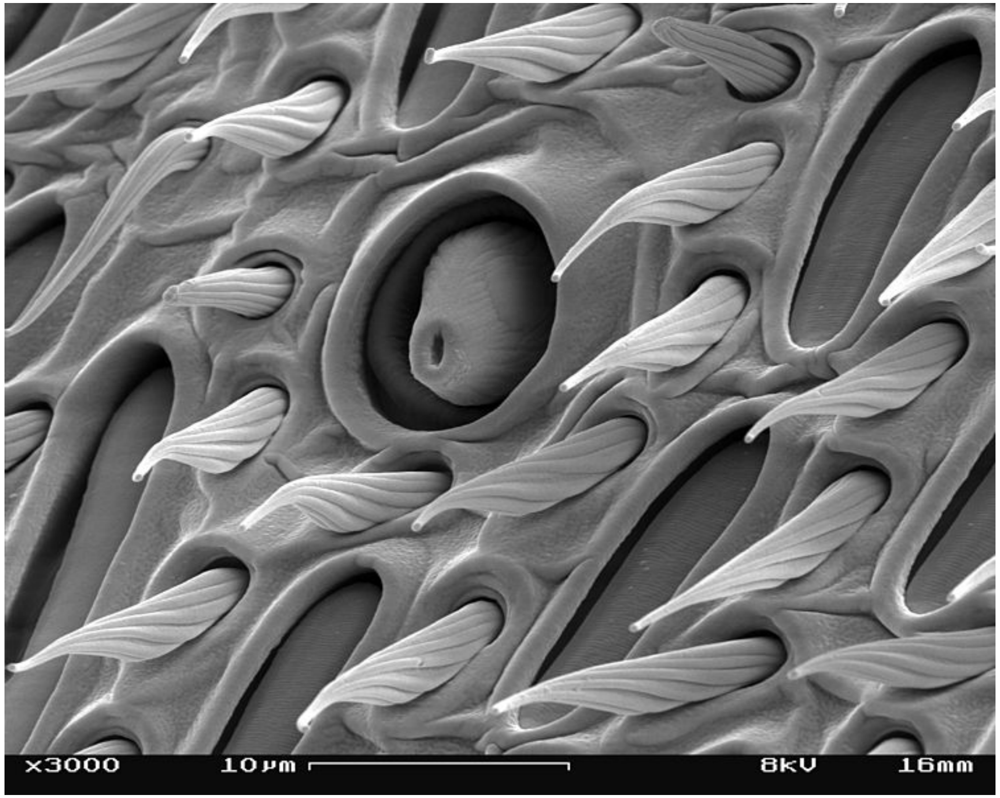

Antenna of common wasp, Vespula vulgaris, wikicommons.

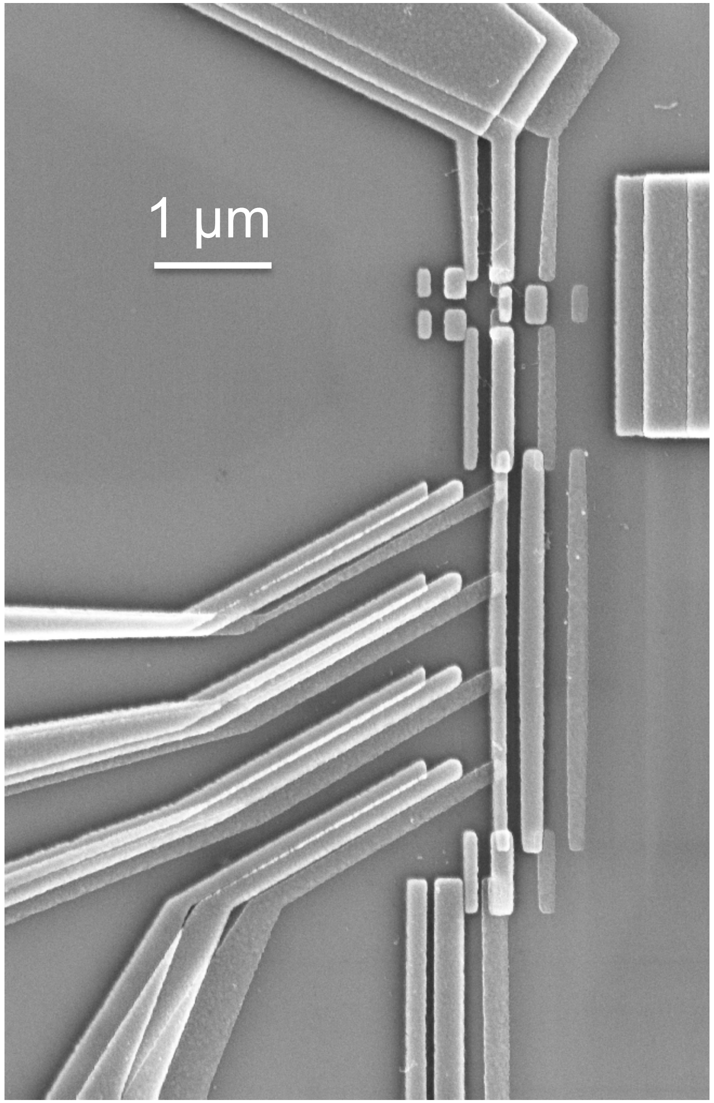

Quantum device for heat transport measurement. B. Dutta et al, Institut Néel & Aalto Univ.

Transmission Electron Microscopy : TEM

The e^- beam (100-300 keV) is shaped, focused by magnetic lenses, goes **through** the sample.

And either projected or scanned (STEM).

Transmitted e^- are collected to build an image.

e^- wavelength 10 pm = 0.1 Å defines the ultimate resolution.

Restricted to transparent samples:
need for delicate sample preparation.
Under vacuum.

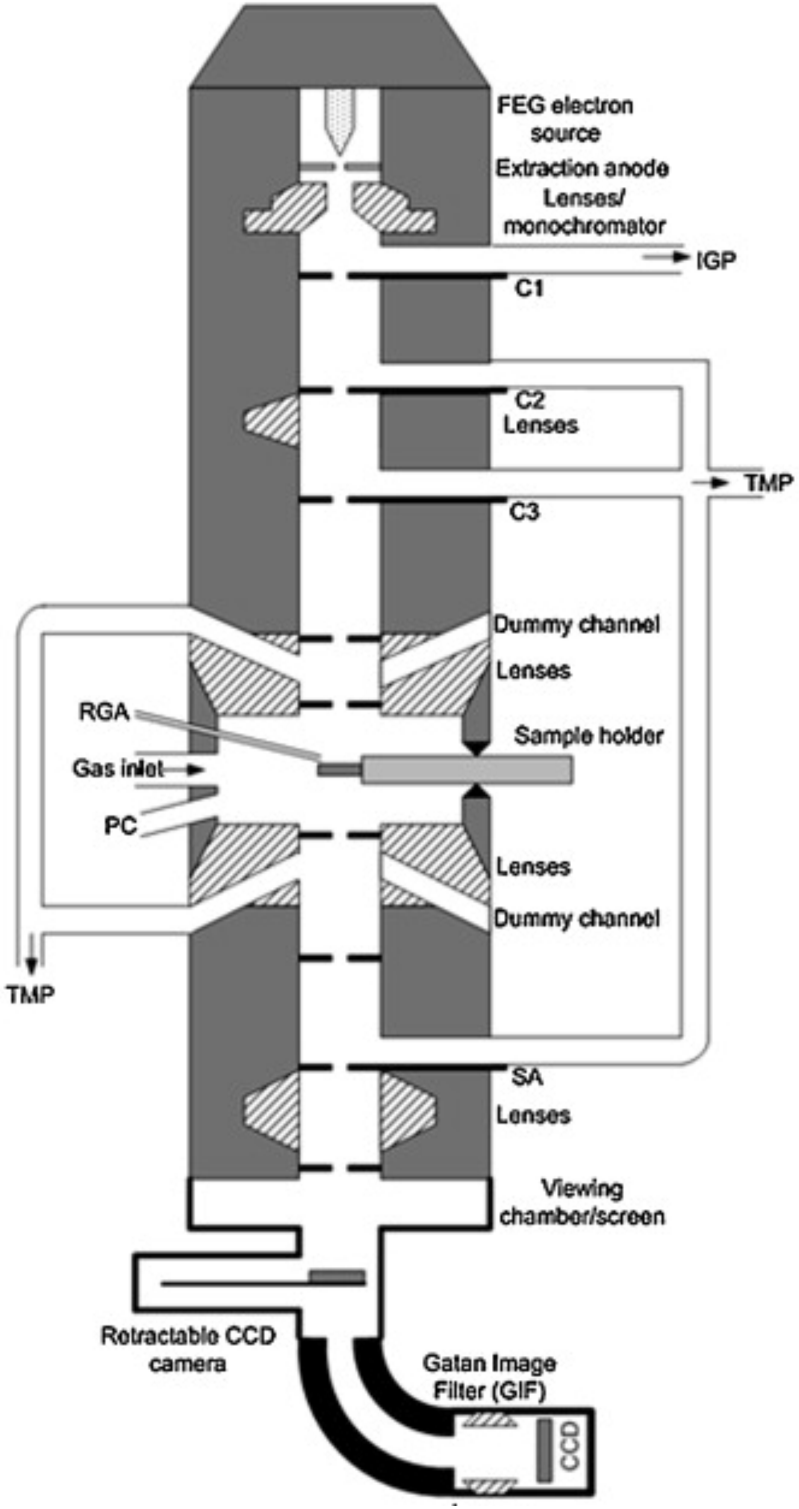

TEM images

TEM lamella preparation

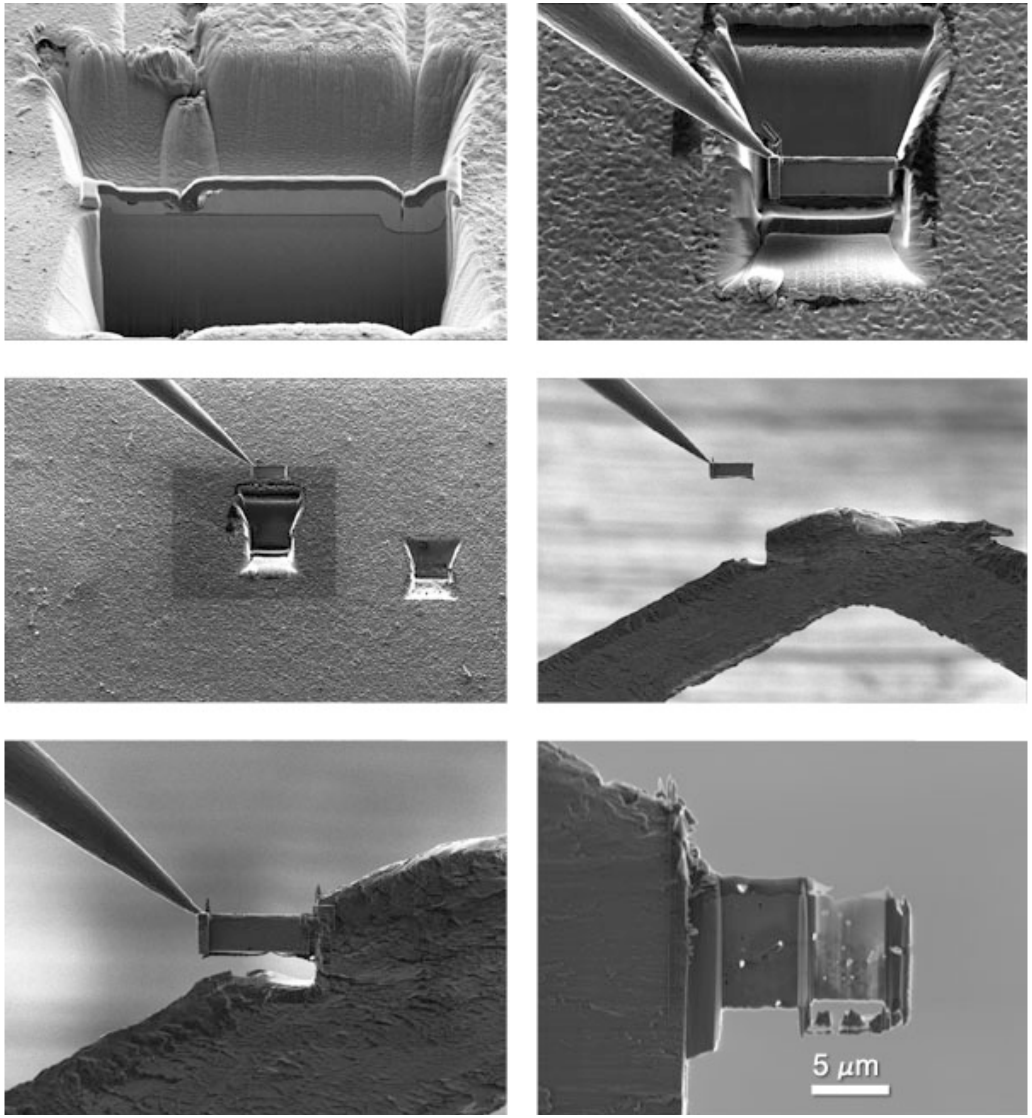

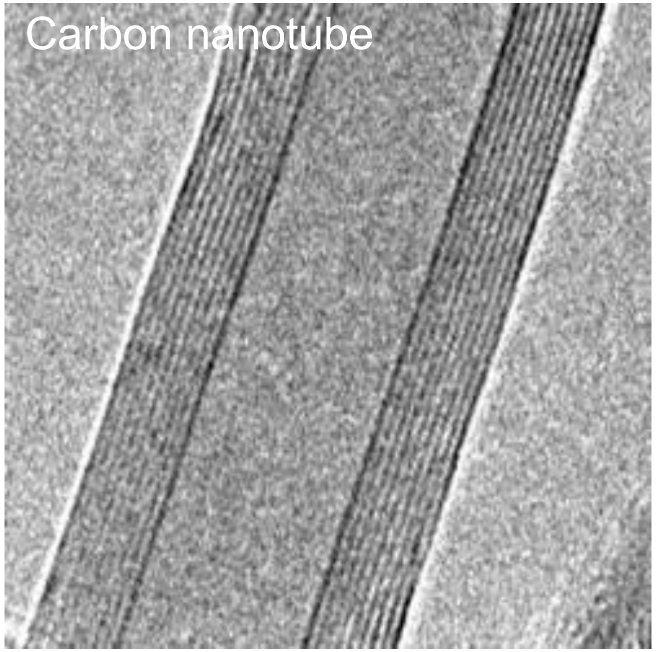

http://www.nano-lab.com

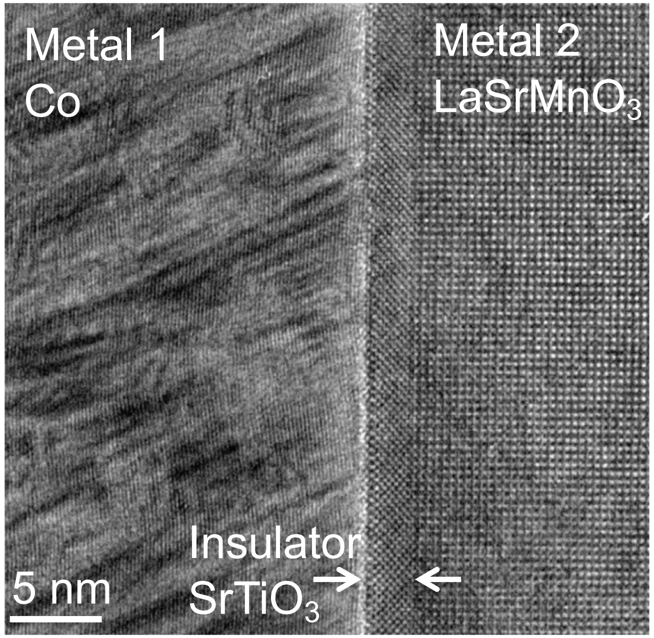

R. Lyonnet, CNRS/Thales

Two types of electron source

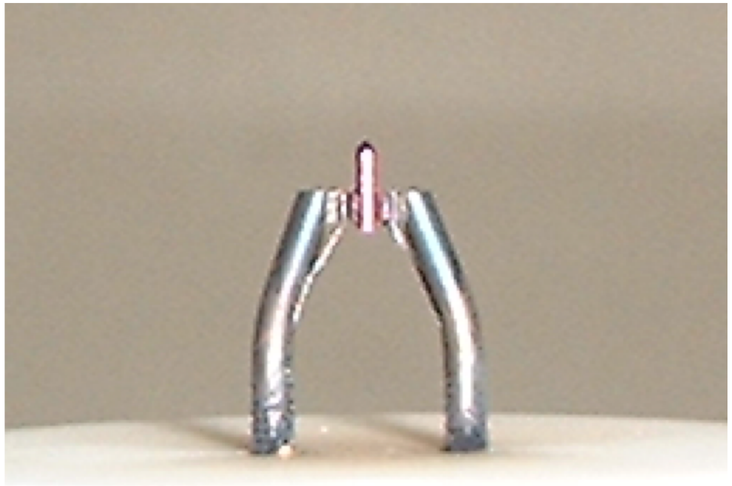

LaB$_6$ filament

Criteria for a good source:
- high current
- small source size
- high stability

Heated filaments: electrons are emitted (thermo-ionic emission) from a heated filament of a material with a high-temperature melting point: W, LaB$_6$

LaB$_6$ lower work-function leads to higher emission.

Degrades with time because of evaporation of the material. Little stable.

Field Emission Gun (FEG): a field applied on a tip extracts electrons.

FESEM: Field Emission Scanning Electron Microscopy

Less energy dispersion

Chapter 1

Tunneling phenomena: from the planar junctions to the STM

Objective: to understand the electron tunnelling effect (including theory), learn the history of STM.

Chapter 1
Tunneling phenomena : from the planar junctions to the STM

1.1: The electronic density of states

The Sommerfeld model of free electrons

Uniform potential for electrons in a metal : free electrons in a box.

Consider their kinetic energy:

$$p = mv = \hbar k \qquad E_c = \frac{(\hbar k)^2}{2m}$$

(k = wave-vector)

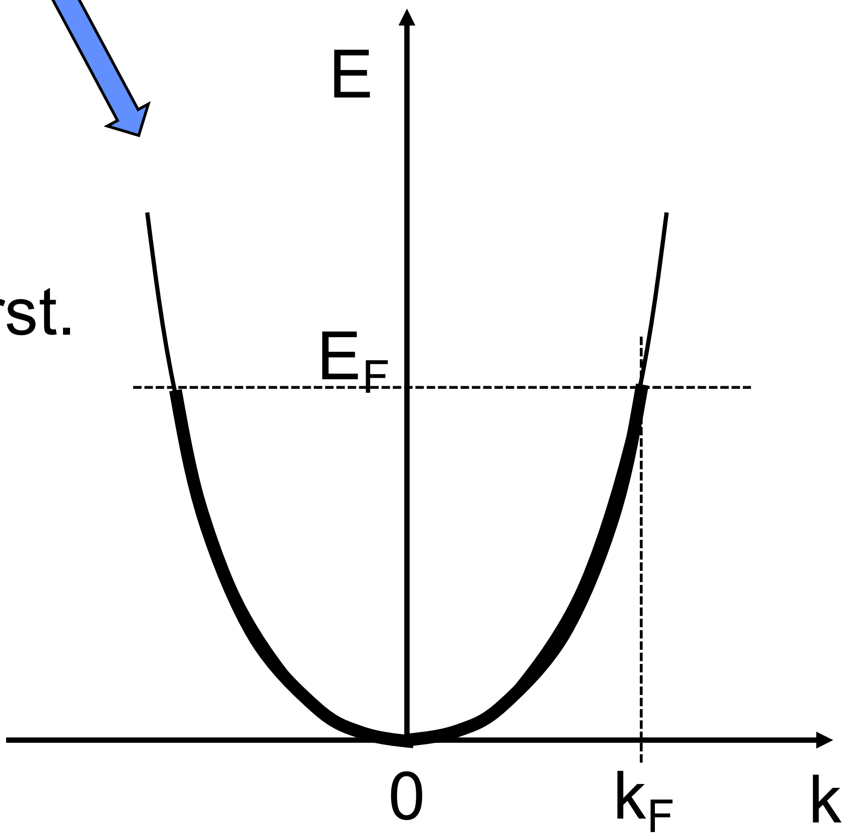

Pauli exclusion principle for Fermions: only two electrons per state (opposite spins).

Electrons occupy states of lowest energy first.

Fermi level = last occupied state at T = 0.

Fermi energy E_F close to electron chemical potential μ:

$$\mu = E_F\left(1 - \frac{\pi^2}{12}\frac{(k_B T)^2}{E_F^2}\right)$$

Counting electron states (1)

Boundary conditions for electrons in a box of dimensions L_x, L_y, L_z:
Wave-function is zero (has a node) at every surface.

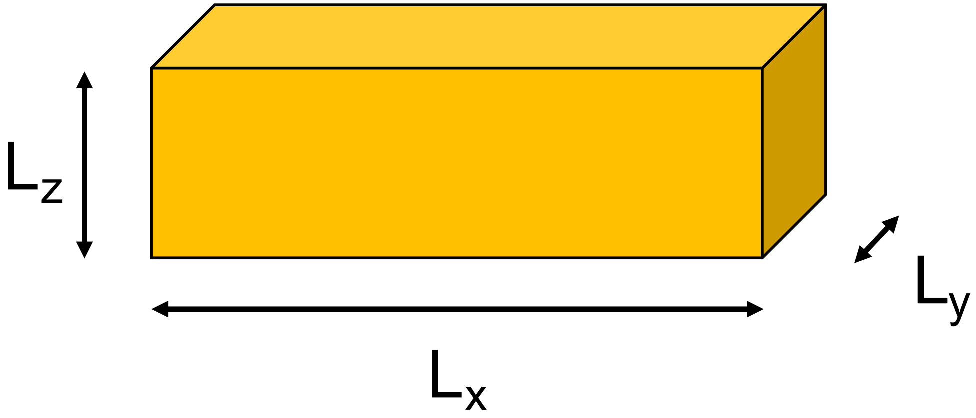

$$k_x = \frac{2\pi m_x}{L_x}; k_y = \frac{2\pi m_y}{L_y}; k_z = \frac{2\pi m_z}{L_z}$$

m_x, m_y, m_z are integers

Counting electron states (2)

An energy below E_F means a wave-vector magnitude below k_F.

Number of states in the **k-space** inside the Fermi sphere of radius k_F ?

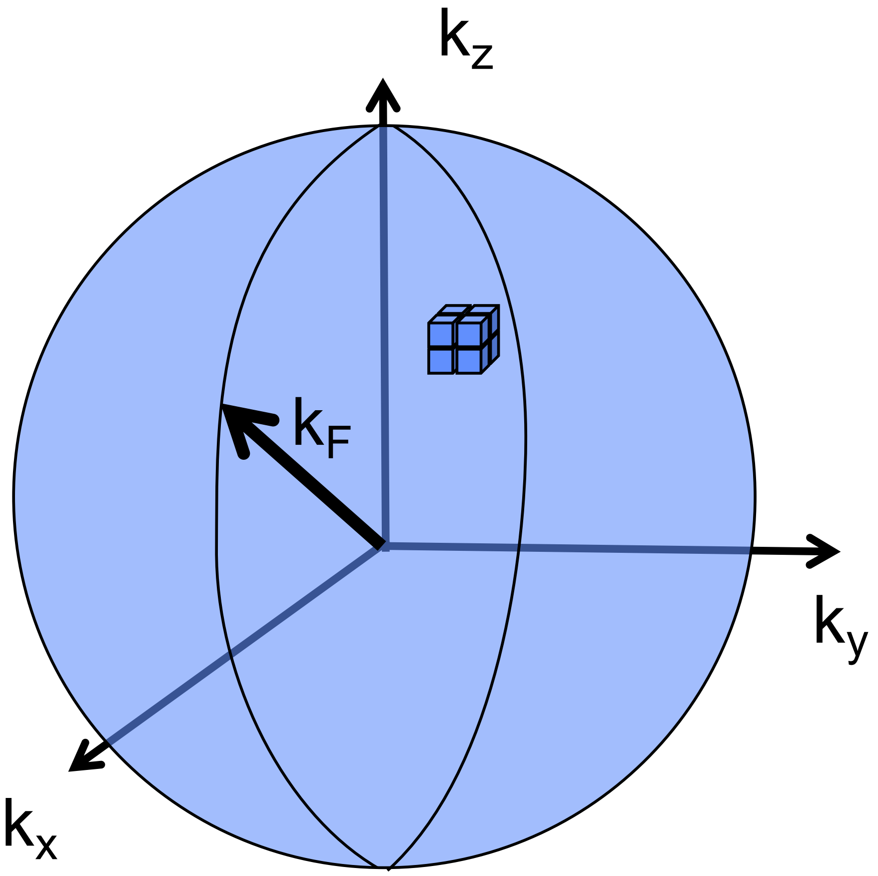

One state is defined by the integers m_x, m_y, m_z

$$k_x = \frac{2\pi m_x}{L_x}; k_y = \frac{2\pi m_y}{L_y}; k_z = \frac{2\pi m_z}{L_z}$$

One state occupies a parallepiped of volume $(2\pi)^3/L_xL_yL_z$.

Counting electron states (3)

Number of states within the Fermi sphere:

$$\underset{\text{spin}\nearrow}{2}\frac{4\pi k_F^3/3}{(2\pi)^3/L_xL_yL_z} = \frac{V}{3\pi^2}k_F^3 = n_F \quad \Rightarrow \quad k_F = \left(\frac{3\pi^2 n_F}{V}\right)^{1/3}$$

n = number of electrons in a metal of volume V, Fermi wave-vector k_F.

The Fermi energy is then: $$E_F = \frac{(\hbar k_F)^2}{2m} = \frac{\hbar^2}{2m}\left(\frac{3\pi^2 n_F}{V}\right)^{2/3}$$

Number of electrons with an energy below E in a volume V:

$$n(E) = \frac{V}{3\pi^2}\left(\frac{2mE}{\hbar^2}\right)^{3/2}$$

The electronic density of states

The electronic Density Of States (DOS) gives the number of states per unit volume and unit energy at a given energy E:

$$\boxed{N(E) = \frac{1}{V}\frac{dn(E)}{dE}}$$

In energy window of width dE, we have dN states per unit volume:

$$\boxed{dN = N(E)\,dE}$$

In a free electrons model, we have: $N(E) = \frac{m}{\hbar^2\pi^2}\sqrt{\frac{2mE}{\hbar^2}}$

“Good” metals

In a free electrons model, we have: $$N(E) = \frac{m}{\hbar^2 \pi^2}\sqrt{\frac{2mE}{\hbar^2}}$$

Varies slowly with energy $$\frac{dN}{N} = \frac{dE}{2E_F}$$

dE is eV, $k_B T$

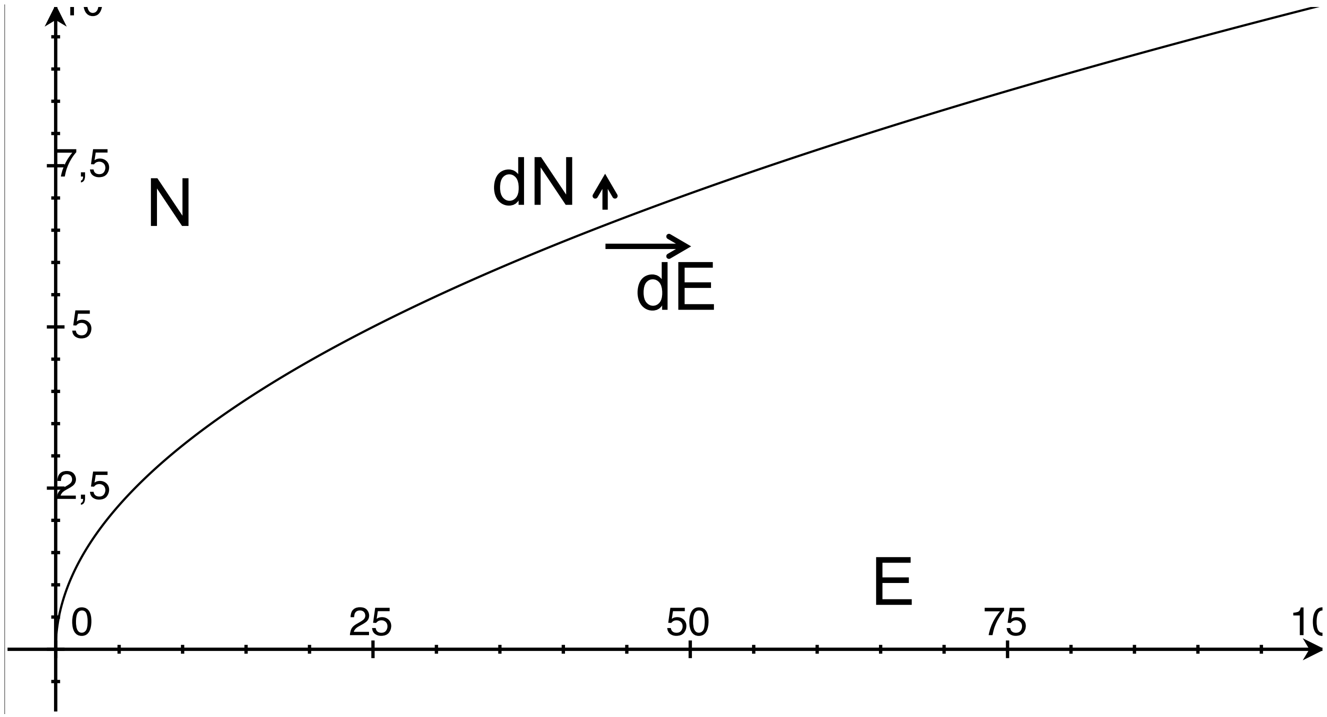

“Real“ materials

DOS in “real“ materials usually differ from the free electrons model expression.

The DOS can vary with the position: one defines the Local Density Of States: LDOS.

With a local tunnel probe, one gets the LDOS.

Chapter 1

Tunneling phenomena : from the planar junctions to the STM

1.2: The electronic work-function

The work-function of a metal (1)

Vacuum states are states with the electron out of the metal.

Definition: the work-function W is the energy needed for an electron to leave the metal.

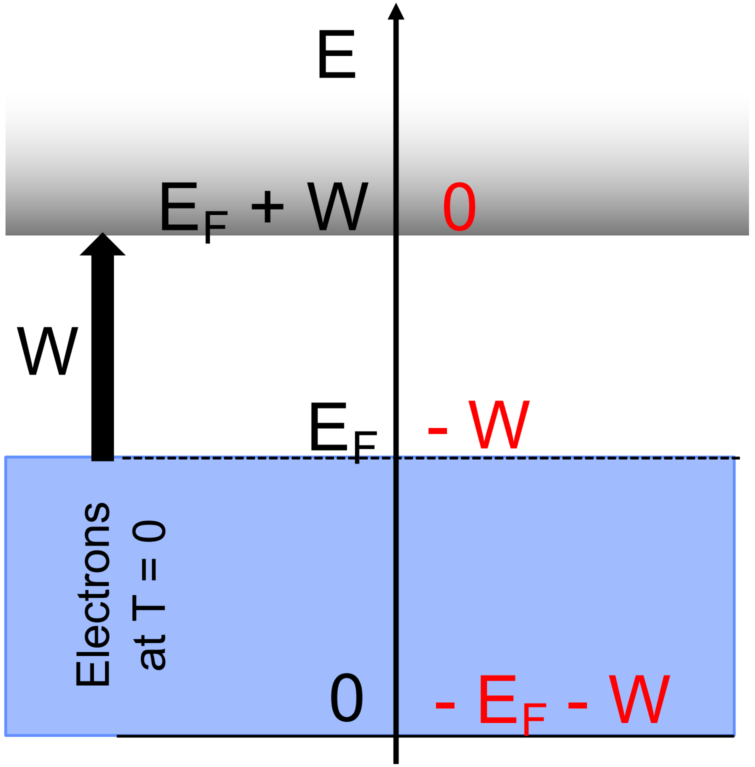

Vacuum states continuum

Fermi level : last occupied electron state at T = 0

Reference energy taken at zero kinetic energy in the metal (black scale), can be chosen also in the vacuum (red), W inchanged.

The work-function of a metal (2)

An electron can by extracted by absorbing a photon: photo-electric effect

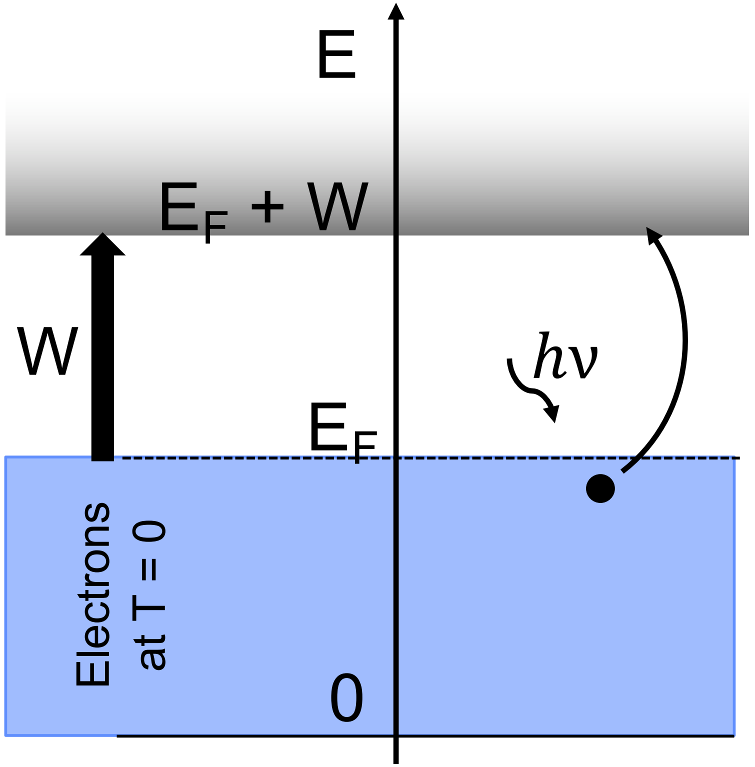

Vacuum states continuum

Fermi level : last occupied electron state at T = 0

The work-function of a metal (3)

Photo-electric effect: the photon hypothesis of Planck confirmed.

Frequency threshold for the photoelectric effect: $h\nu = W$

No current if: $eU_0 = h.\nu - W$

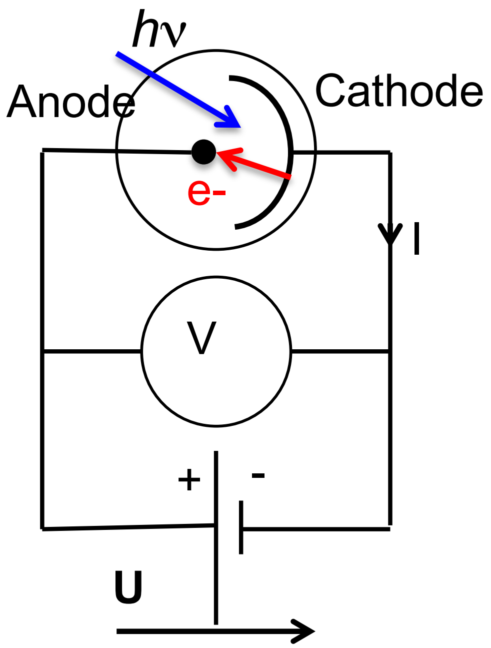

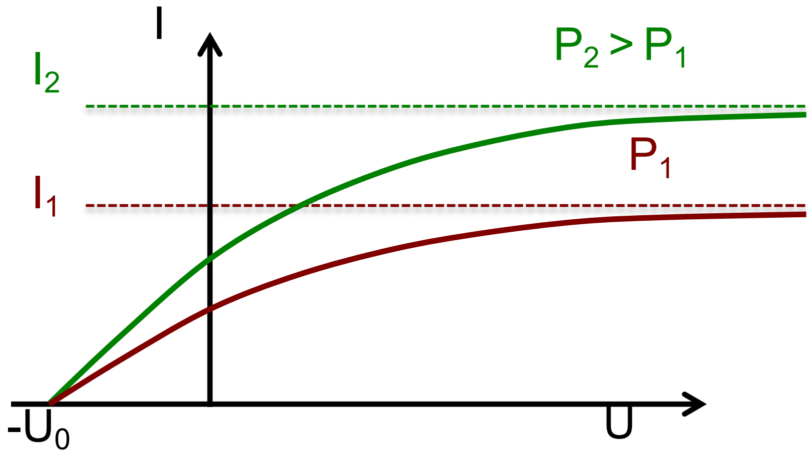

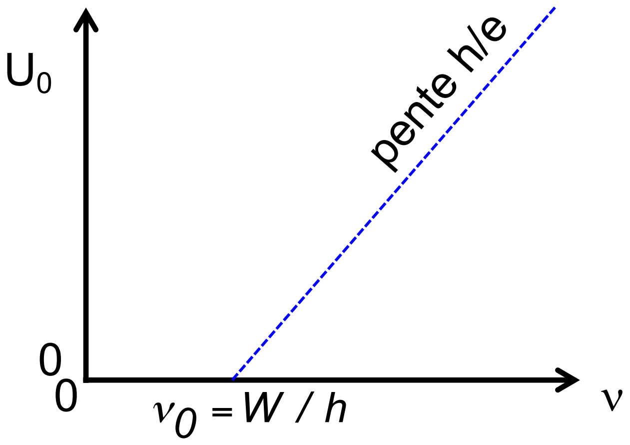

The work-function of a metal (2)

If temperature is very high, high-energy electrons can escape.

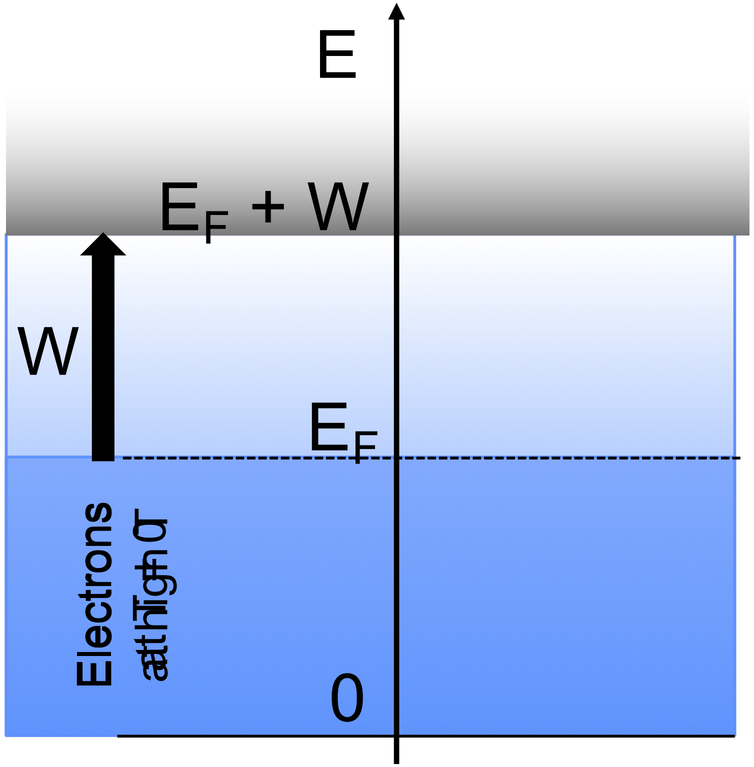

Vacuum states continuum

Fermi level : last occupied electron state at T = 0

Thermo-ionic emission

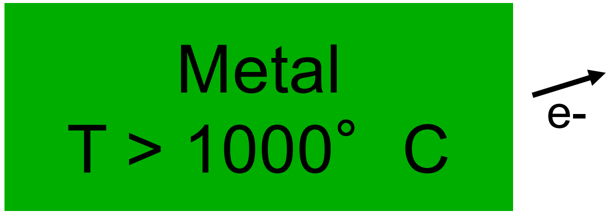

Metal

T > 1000° C

e-

Current density: $$j \propto T^2 \exp\left(-\frac{W}{k_B T}\right)$$

Used in e- beam source in SEM, evaporators

Measurement of the work-function

- Photo-electric effect

- Thermo-ionic emission

- Kelvin probe (see Part II)

Values :

Metal	W (eV)
Li	2.38
LaB_6	2.5
Cu	4.4
Au	4.3
Hg	4.52
Al	4.25
W	4.5

Chapter 1
Tunneling phenomena: from the planar junctions to the STM

1.3: The basic “square barrier model“

The square barrier model

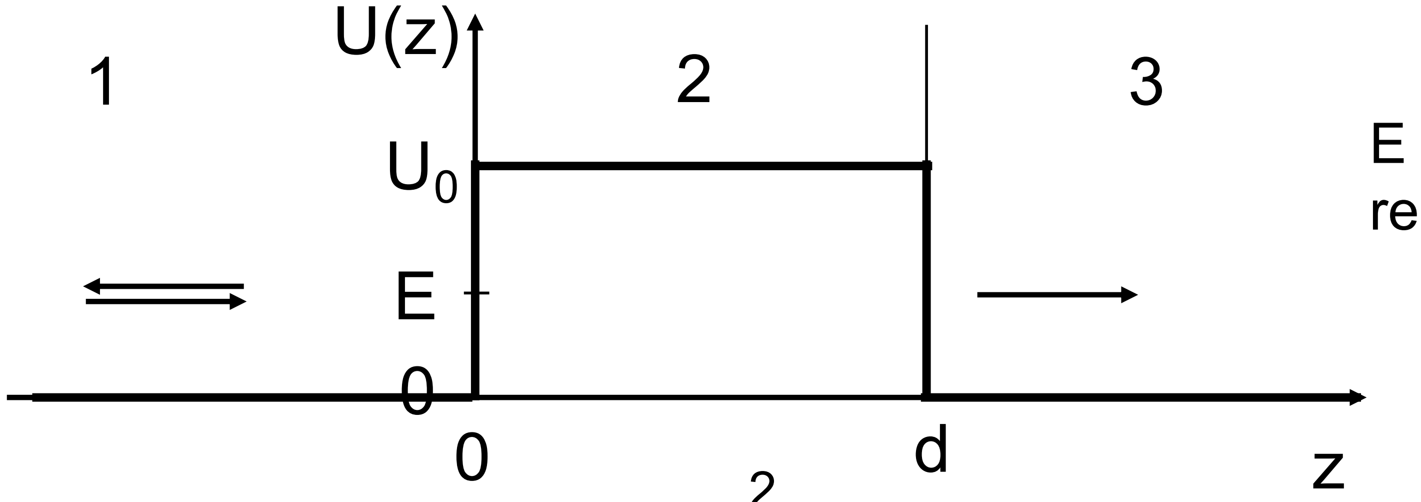

E = kinetic energy in region 1, where U = 0

Classical mechanics : $\frac{p_z^2}{2m} + U(z) = E$

One needs E > U(z) for the e^- to sit at a given point.
If E < W, the e^- stays in region 1.

Quantum mechanics : wave-function description satisfying the Shrödinger equation

$$\frac{-\hbar^2}{2m}\frac{d^2\psi}{dz^2} + U(z)\psi(z) = E\psi(z)$$

The particle current

Density of probability of presence is: $\rho = \left|\psi\right|^2$

The particle current defined as: $\vec{j} = \frac{-i\hbar}{2m}\left[\psi^* \vec{\nabla}\psi - \psi\vec{\nabla}\psi^*\right]$

obeys the conservation law: $\frac{\partial\rho}{\partial t} + \mathrm{div}\ \vec{j} = 0$

Simple case, the plane wave: $\psi\left(x\right) = A\ e^{ikx}$

The particle current is then: $\vec{j} = \frac{\hbar\vec{k}}{m}\left|A\right|^2 = \vec{v}\left|A\right|^2$

The square barrier transmission

In 1 (z < 0): $\psi_1(z) = e^{ikz} + A \, . \, e^{-ikz}$ where $k = \frac{\sqrt{2mE}}{\hbar}$

In 2 (0 < z < d): $\psi_2(z) = B \, . \, e^{\alpha z} + C \, . \, e^{-\alpha z}$ where $\alpha = \frac{\sqrt{2m(U_0 - E)}}{\hbar}$

In 3 (d < z): $\psi_3(z) = De^{ikz}$

Continuity of ψ and its spatial derivative $d\psi/dz$:
4 equations provide the determination of A, B, C and D.

The transmission coefficient is: $T = \left|\frac{D}{1}\right|^2 = \frac{1}{1 + \frac{U_0^2}{4E(U_0 - E)} sh^2(\alpha d)}$

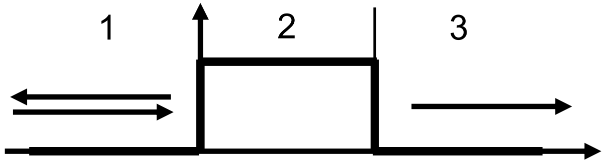

Overlapping wavefunctions

A misleading drawing that is often shown:
what does the red line display ??

In 1 (z < 0): $\psi_1(z) = e^{ikz} + A \,.\, e^{-ikz}$ where $k = \frac{\sqrt{2mE}}{\hbar}$

In 2 (0 < z < d): $\psi_2(z) = B \,.\, e^{\alpha z} + C \,.\, e^{-\alpha z}$ where $\alpha = \frac{\sqrt{2m(U_0 - E)}}{\hbar}$

In 3 (d < z): $\psi_3(z) = De^{ikz}$

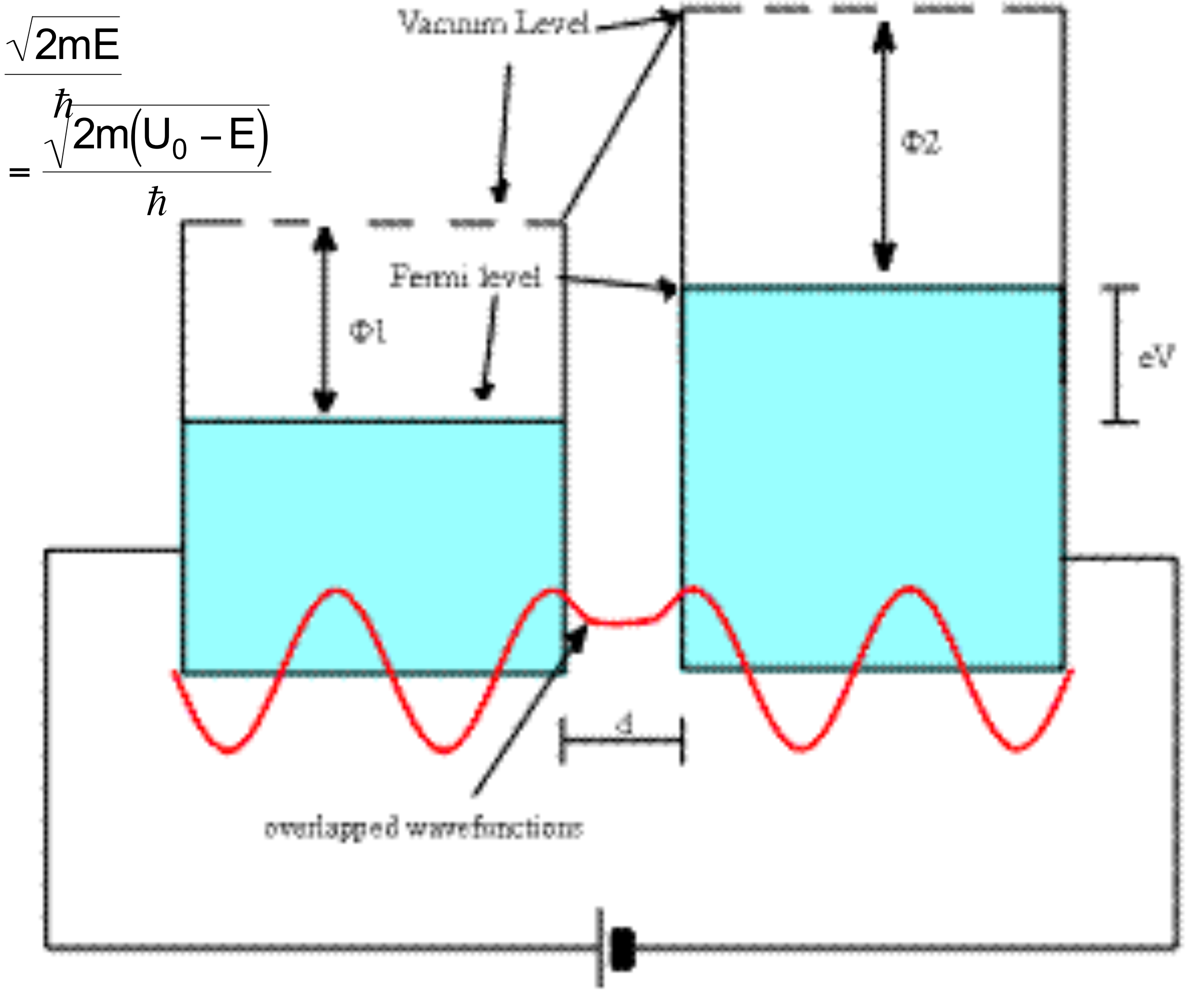

The thick barrier approximation

$$T = \left|\frac{D}{1}\right|^2 = \frac{1}{1 + \frac{U_0^2}{4E\left(U_0 - E\right)} \mathrm{sh}^2\left(\alpha d\right)}$$

Thick barrier approximation ($\alpha d >> 1$):

$$T \approx 16 \frac{E\left(U_0 - E\right)}{U_0{}^2} e^{-2\alpha d}$$

Exponential decay of the transmission amplitude:

$$\boxed{T \propto \exp\left(-2\alpha d\right)}$$

A first order of magnitude

Order of magnitude: a man of mass m = 100 kg, a wall h = 4 m high, thickness = d

Energy barrier = mgh

$$T = \exp\left(-2\frac{\sqrt{2.100.100.9,81.4}}{1,05.10^{-34}}d\right) = \exp\left(-2.10^{37}d\right)$$

T vanishing even with d down to Å scale.

The case of electrons

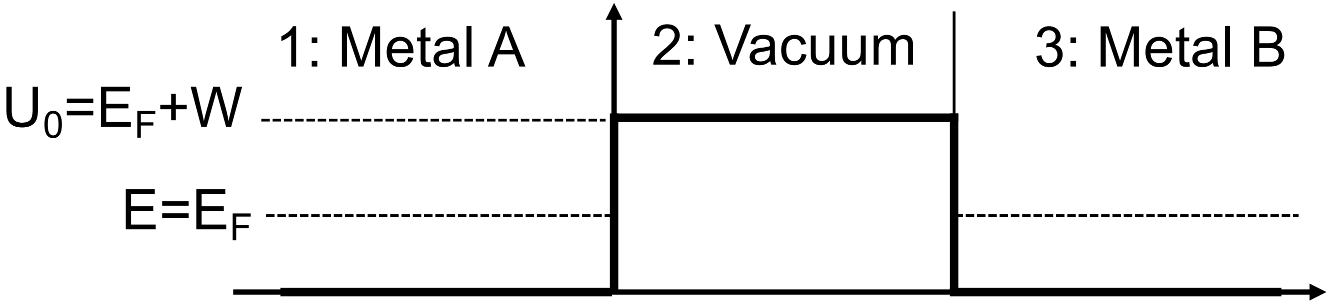

$$E \approx E_F$$
$$U_0 = E_F + W$$

$$\Rightarrow \quad \alpha = \frac{\sqrt{2mW}}{\hbar} \qquad T \approx 16\frac{E_F W}{\left(E_F + W\right)^2} e^{-2\alpha d} \propto \exp\left(-2\alpha d\right)$$

$$T = \exp\left(-2\frac{\sqrt{2.9,1.10^{-31}.4.1,6.10^{-19}}}{1,05.10^{-34}} d\right) = \exp\left(-2.10^{10} d\right)$$

Thanks to the low electron mass and low energy barrier:

T is non negligible for d of the order of the Å.

Tunneling vs conduction

This slide is out of the scope of the present lecture, and here only to make the connection with the field of quantum/mesoscopic transport.

How large can a tunnel current be ?

Mesoscopic transport: $$I = G_Q V \sum_{\text{channel } i} T_i$$

Quantum conductance: $$G_Q = \frac{2e^2}{h} = \frac{1}{12.9\,\mathrm{k}\Omega}$$ (includes spin)

Diffusive transport: T is close to 1.

Tunnel effect: T is “small“.

With $V = 0.13$ V, $T = 10^{-4}$ for one channel: $I = 1$ nA

Transmission through an arbitrary barrier

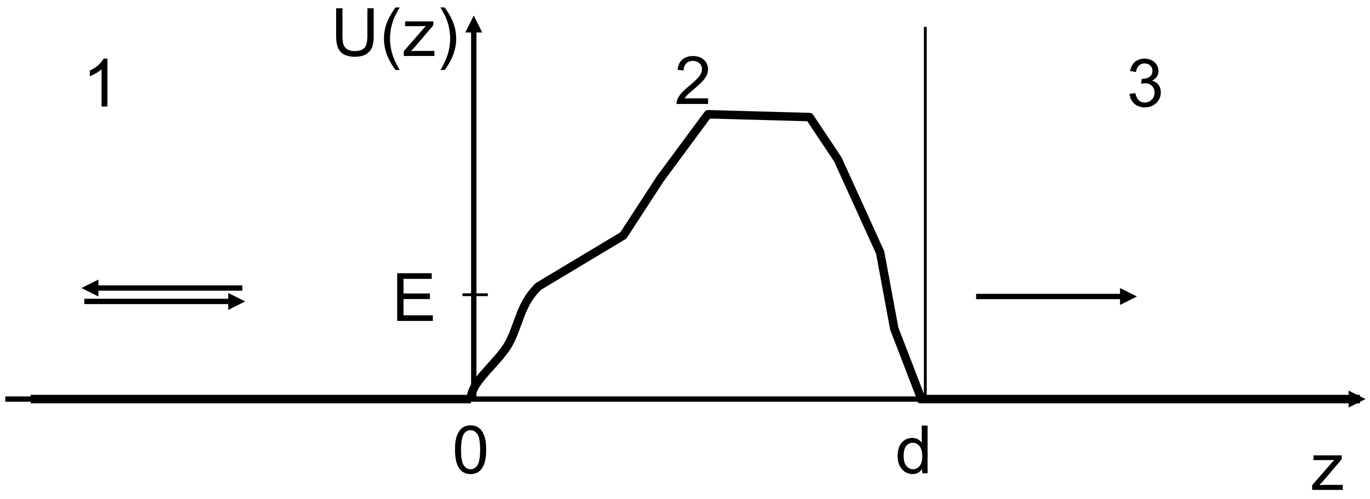

WKB (Wentzel, Kramers and Brillouin) semiclassical approximation (slow spatial variation of the wave-function amplitude, no local minima).

Arbitrary barrier: WKB result interpretation

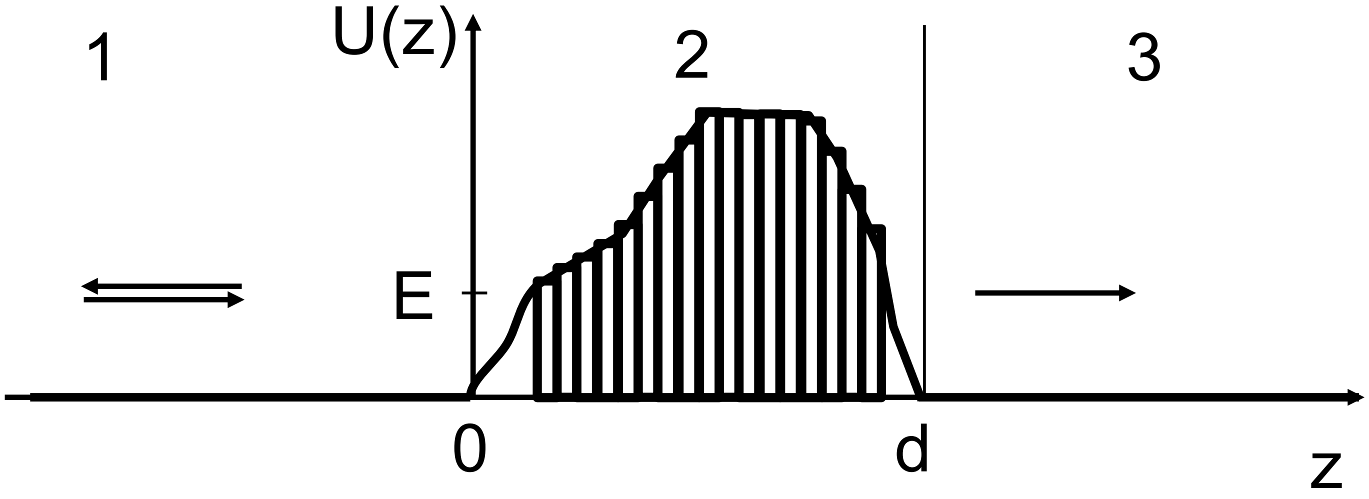

Decomposition of the barrier into square (rectangular) barriers, local height $U(z_i)$, width dz:

$$T_i \propto \exp\left(-\frac{2}{\hbar}\left[2m\left(U\left(z_i\right)-E\right)\right]^{1/2}dz\right)$$

Total transmission: $T = \prod T_i \propto \prod \exp\left(-\frac{2}{\hbar}\left[2m\left(U\left(z_i\right)-E\right)\right]^{1/2}dz\right)$

$$T \propto \exp\left(-\frac{2}{\hbar}\sum\left[2m\left(U\left(z_i\right)-E\right)\right]^{1/2}dz\right) \approx \exp\left(-\frac{2}{\hbar}\int_{U>E}\left\{\left[2m\left(U\left(z\right)-E\right)\right]^{1/2}dz\right\}\right)$$

Transmission through an arbitrary barrier

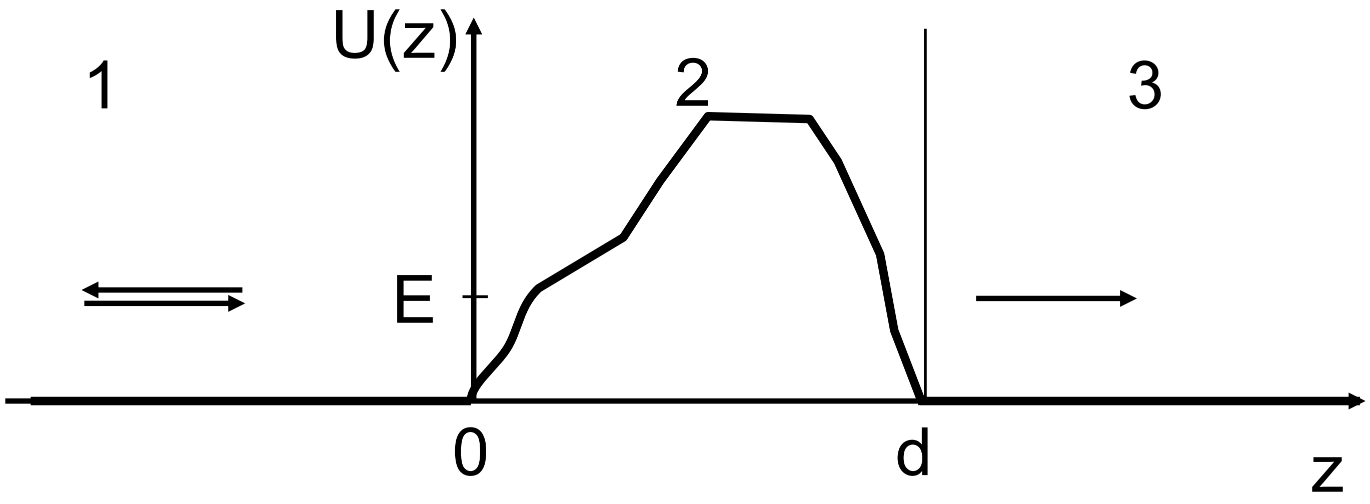

WKB result:

$$\boxed{T \propto \exp\left(-\frac{2}{\hbar}\int_{U>E}\left\{\left[2m\left(U\left(z\right)-E\right)\right]^{1/2}dz\right\}\right)}$$

Coincides with barrier model result in this special case.

Chapter 1
Tunneling phenomena: from the planar junctions to the STM

1.4: A microscopic picture

Microscopic view

Tunnel matrix element describes the overlap of the electronic wave-functions:

$$\boxed{M_{\psi\chi} = \iint_S \left(\chi^* \frac{\partial\psi}{\partial z} - \psi \frac{\partial\chi^*}{\partial z} \right) dS}$$

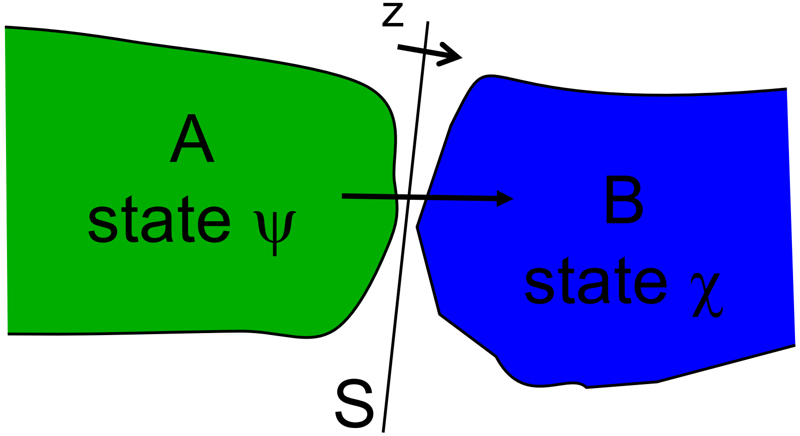

Hypothesis: Electron states χ and ψ are not affected by the tunnel contact.
Bardeen, 1964

Integral over any surface S in the vacuum between the two metals, depends obviously on distance between A and B.

Tunneling probability

The Fermi golden rule gives the transition probability from a state ψ to a state χ:

$$\boxed{p_{\psi\to\chi} = \frac{2\pi}{\hbar}\left|\langle\psi|H_T|\chi\rangle\right|^2\delta\left(E_\psi - E\chi\right) = \frac{2\pi}{\hbar}\left|M_{\psi\chi}\right|^2\delta\left(E_\psi - E\chi\right)}$$

Valid for every couple of states (state in metal A, state in metal B).

The $\mathrm{I}M_{\psi\chi}\mathrm{I}^2$ term includes the distance dependence.

The tunneling effect is elastic to first order (no energy exchange). Inelastic tunneling rate is only about 10^{-5} of the elastic rate.

$\delta(x)$ = Dirac delta function (= 0 except if x = 0).

$$\int_{-\infty}^{+\infty} f(x)\delta(x) = f(0)$$

Chapter 1

Tunneling phenomena: from the planar junctions to the STM

1.5: The tunneling current

the two following parts are the most theoretical ones of the lecture

Two metals

Two metals far away: we plot the DOS, occupied states at T = 0 are colored.

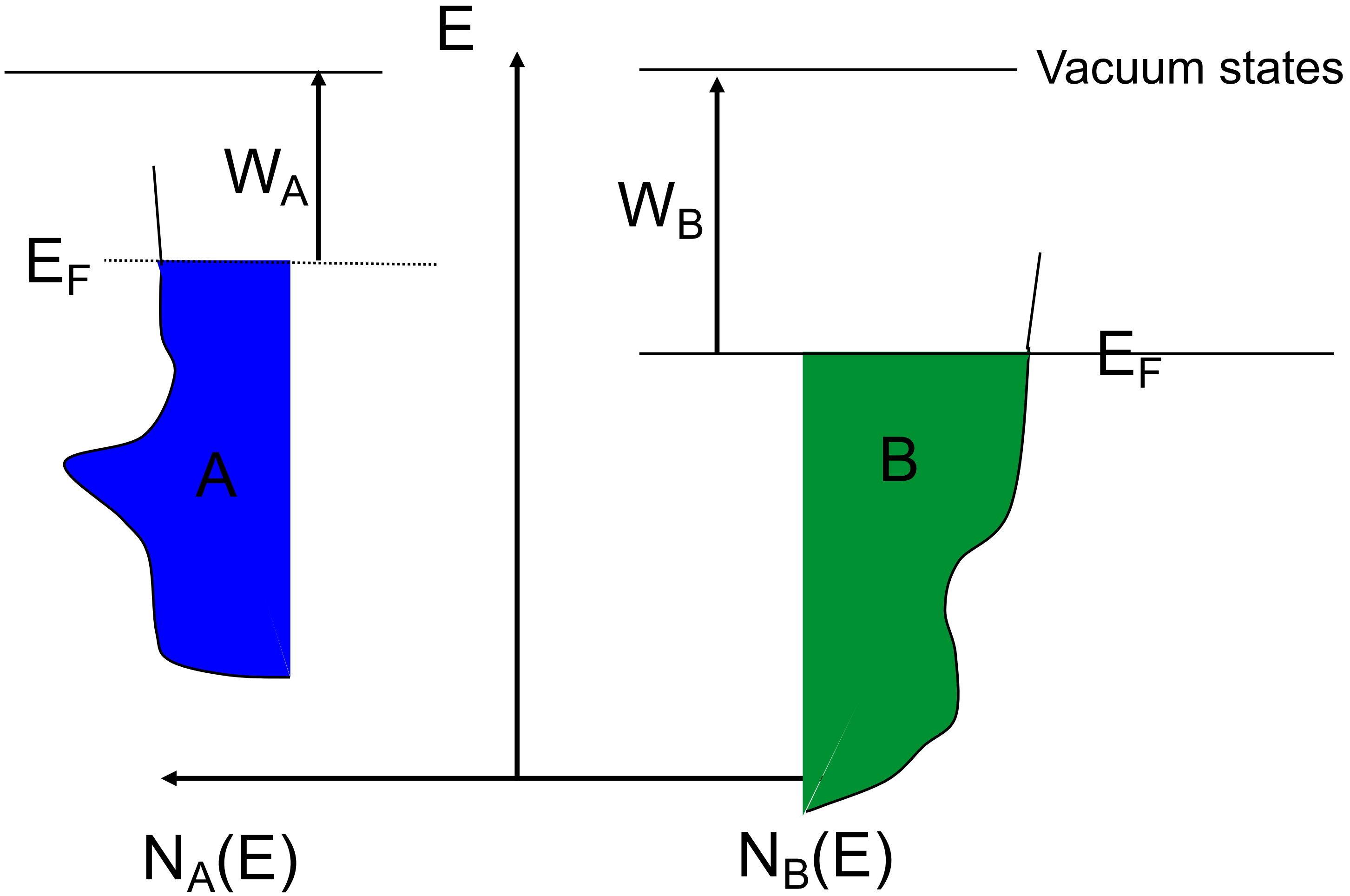

N_A, N_B: Local Density Of (electronic) States (LDOS) of metal A or B.

Work-functions W_A, W_B can be different.

Equilibrium situation

Consider two metals at zero bias, the two FL get aligned.

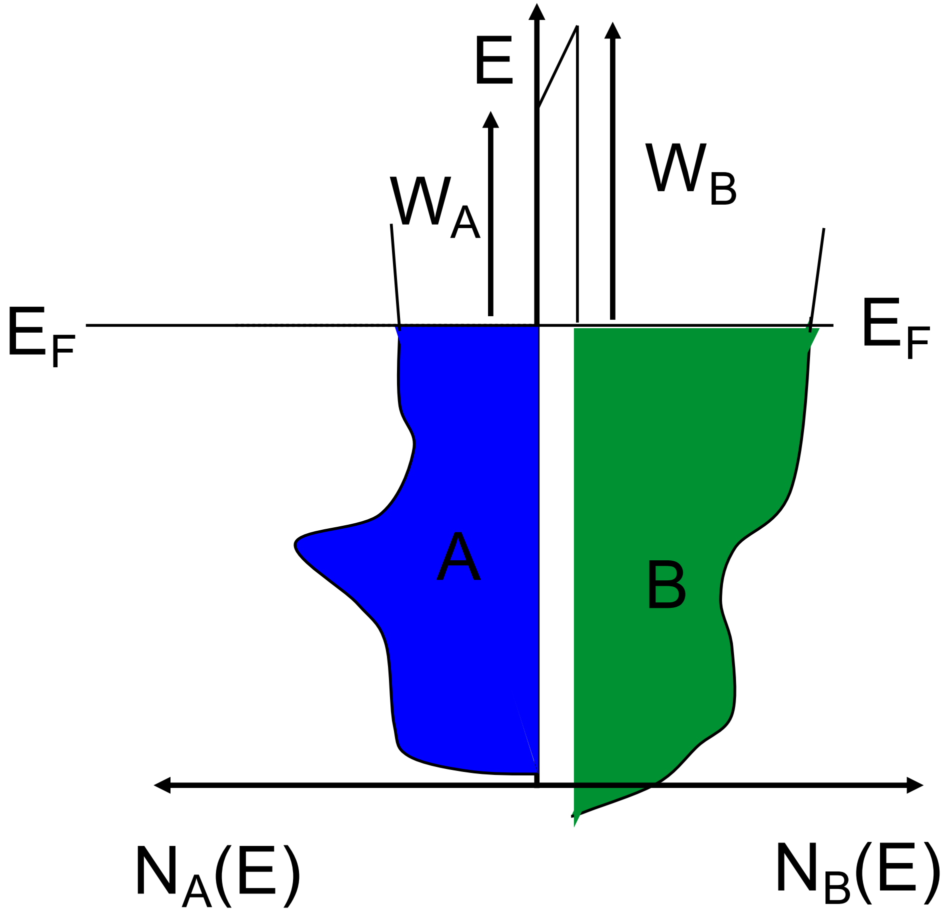

N_A, N_B: Local Density Of (electronic) States (LDOS) of metal A or B.

If different work-functions $W_A \neq W_B$:

non-zero electric field between the metals, cf KFM.

With a voltage bias

Consider two metals with a voltage bias in-between.

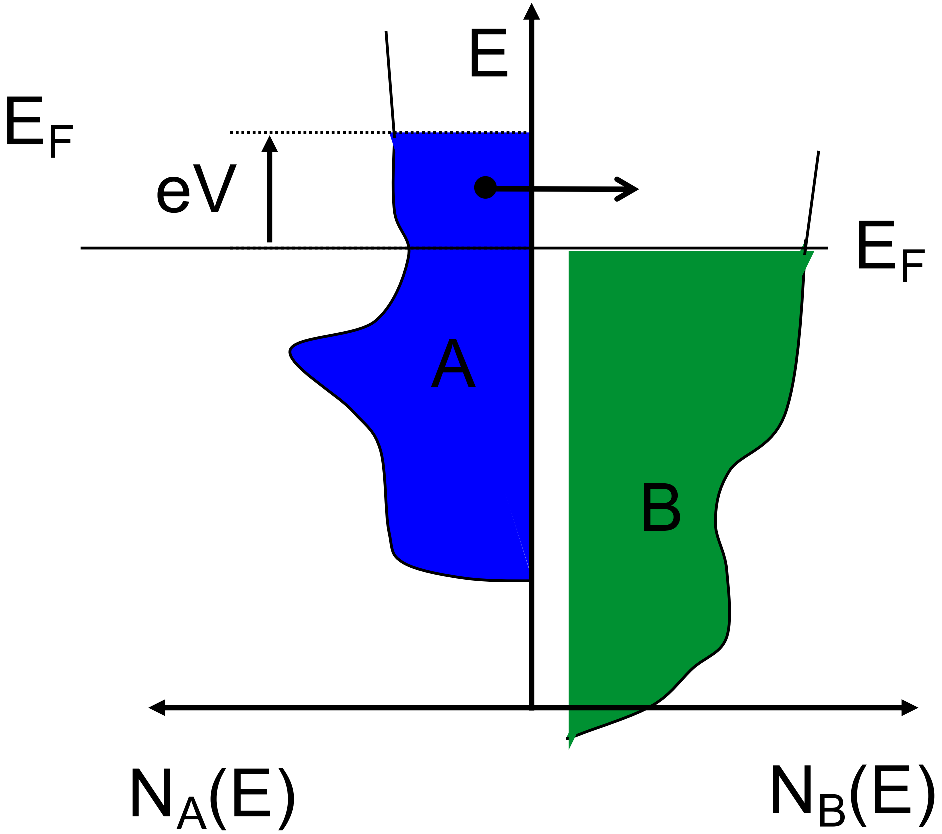

N_A, N_B: Local Density Of (electronic) States (LDOS) of metal A or B.

Voltage bias V: shifts the FLs.

$N_A(E) \Rightarrow N_A(E-eV)$

Elastic electron tunneling:

“Horizontal” process.

Electron energy relaxation

After the electron is transmitted, it **will** relax to lower energy

Thanks to inelastic processes with e-, phonons, …

Separate process from tunneling, much longer times involved.

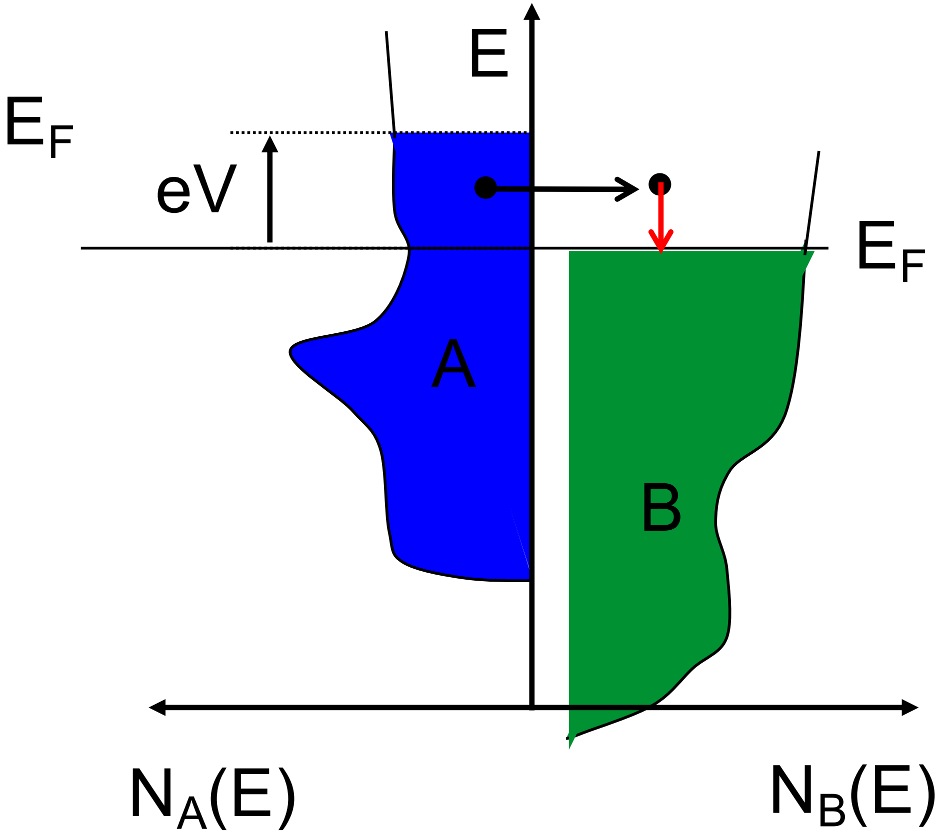

Doping / biasing

Biasing = adding a potential, E_F does not move compared to DOS.

Doping = adding/removing electrons, E_F moves compared to DOS.

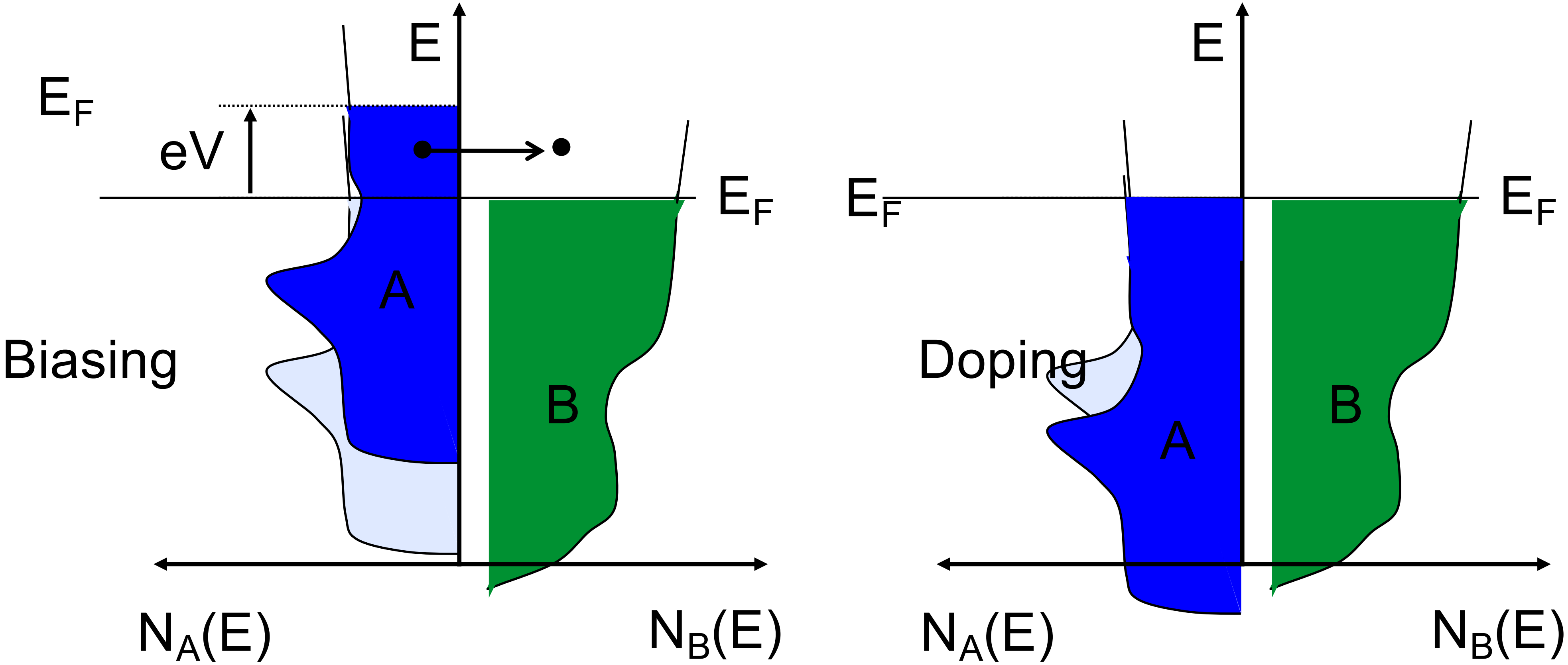

The energy distribution function

Non-zero temperature: the energy distribution function f(E) gives the probability for an e^- state at the energy E to be occupied.

At thermal equilibrium, f is the Fermi-Dirac function:

$$f(E) = \frac{1}{1 + \exp\left[\frac{E - E_F}{k_B T}\right]}$$

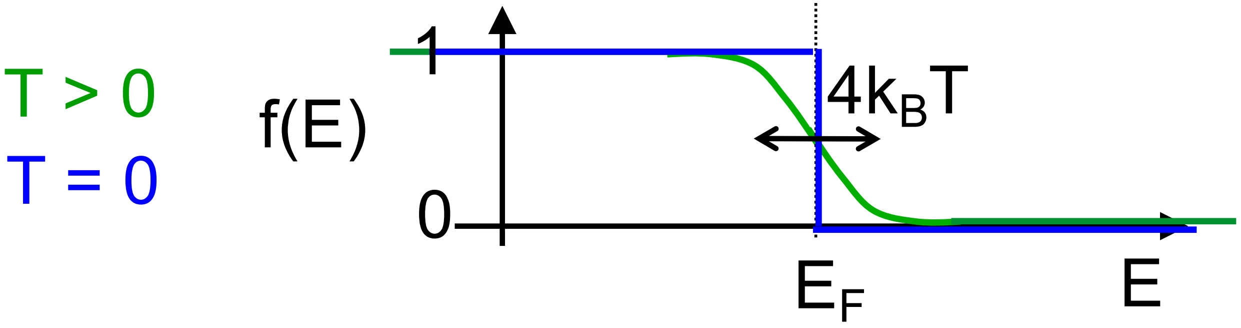

$f(E_F) : 1/2$

At zero temperature, it reduces to a step function.

Relaxation towards eq. distribution through inelastic scattering: e-e, e-ph

At non-zero temperature

Non-zero temperature, the number of electrons for a given spin within a window dE at an energy E is:

$$\boxed{dN = N(E)\, f(E) dE}$$

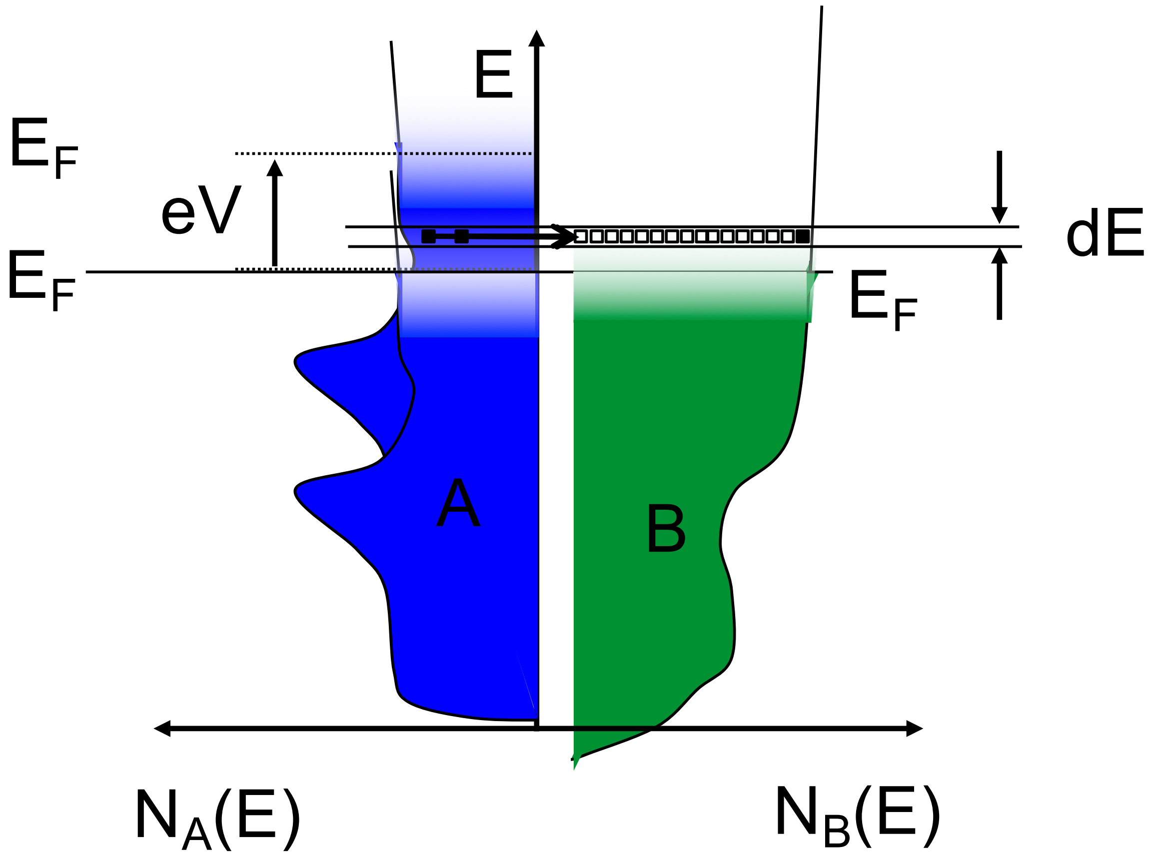

Consider an energy window [E;E+dE] and determine the electron flow from A to B.

The tunnel current expression (1)

What's the electron flow from A to B ?

Number of occupied states in A at the energy E = $N_A(E-eV)f(E-eV)dE$

Number of free states in B at the energy E'= $N_B(E')[1-f(E')]dE'$

Tunnel current element (Fermi golden rule):

$$d^2I_{A\to B} = \overset{\text{spin}}{2}e\underbrace{\frac{2\pi}{\hbar}|M_{AB}|^2\delta(E-E')}_{p}N_A(E-eV)N_B(E')f(E-eV)[1-f(E')]dEdE'$$

$$dI_{A\to B} = 2e\frac{2\pi}{\hbar}|M_{AB}|^2\int_{E'=-\infty}^{+\infty}\delta(E-E')N_A(E-eV)N_B(E')f(E-eV)[1-f(E')]dEdE'$$

$$dI_{A\to B} = 2e\frac{2\pi}{\hbar}|M_{AB}|^2N_A(E-eV)N_B(E)f(E-eV)[1-f(E)]dE$$

The tunnel current expression (1’)

What’s the electron flow from B to A ?

Number of occupied states in B at the energy E’ = $N_B(E')f(E')dE'$

Number of free states in A at the energy E= $N_A(E-eV)\left[1-f(E-eV)\right]dE$

Tunnel current element (Fermi golden rule):

$$d^2I_{B\to A} = 2e\frac{2\pi}{\hbar}\left|M_{AB}\right|^2\delta(E-E')N_B(E')N_A(E-eV)f(E')\left[1-f(E-eV)\right]dEdE'$$

$$dI_{B\to A} = \frac{4e\pi}{\hbar}\left|M_{AB}\right|^2\int_{E'=-\infty}^{+\infty}\delta(E-E')N_B(E')N_A(E-eV)f(E')\left[1-f(E-eV)\right]dE\,dE'$$

$$dI_{B\to A} = 2e\frac{2\pi}{\hbar}\left|M_{AB}\right|^2 N_B(E)N_A(E-eV)f(E)\left[1-f(E-eV)\right]dE$$

The tunnel current expression (2)

Net current, with the hypothesis that M depends only on E:

$$dI = dI_{A\rightarrow B} - dI_{B\rightarrow A}$$

$$= \frac{4\pi e}{\hbar}\left|M(E)\right|^2 N_A(E-eV)N_B(E)\left\{f(E-eV)\left[1-f(E)\right]-f(E)\left[1-f(E-eV)\right]\right\}dE$$

$$= \frac{4\pi e}{\hbar}\left|M(E)\right|^2 N_A(E-eV)N_B(E)\left[f(E-eV)-f(E)\right]dE$$

Total current :

$$\boxed{I = \int_{-\infty}^{+\infty} dI = \frac{4\pi e}{\hbar}\int_{-\infty}^{+\infty}\left|M(E)\right|^2 N_A(E-eV)N_B(E)\left[f(E-eV)-f(E)\right]dE}$$

Interpretation: a tunnel current occurs because of an electron states occupancy (at a given energy) difference.

The tunnel current expression (3)

$$\boxed{I=\int_{-\infty}^{+\infty} dI=\frac{4\pi e}{\hbar}\int_{-\infty}^{+\infty}\left|M(E)\right|^2 N_A(E-eV)N_B(E)\left[f(E-eV)-f(E)\right]dE}$$

If A (the tip) is a good metal : $N_A(E)$ = Constant.

Hypothesis: M(E) = Constant (eV << W).

$$\boxed{I\propto\int_{-\infty}^{+\infty} N_B(E)\left[f(E-eV)-f(E)\right]dE}$$

Zero temperature tunneling spectroscopy

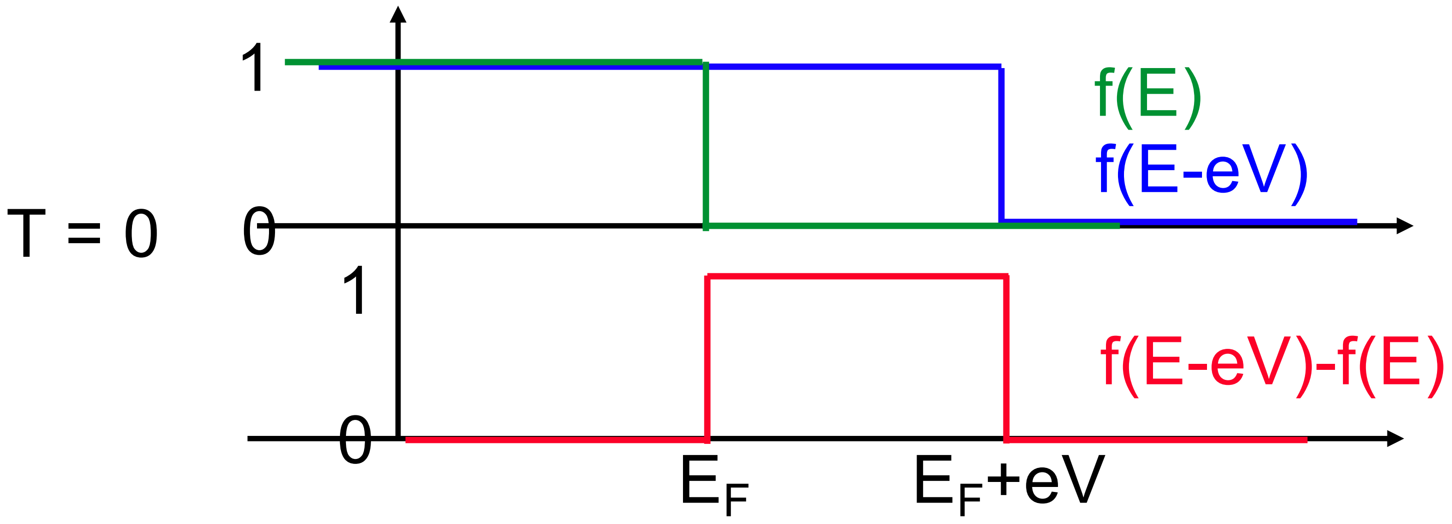

$$I \propto \int_{E_F}^{E_F+eV} N_B(E)\,dE$$

Calculating the derivative with respect to voltage provides the differential conductance, which is a function of voltage bias.

$$\frac{dI}{dV}(V) \propto N_B(E_F + eV)$$

Zero temperature tunneling spectroscopy

The derivative of the current with respect to voltage is the differential conductance, which is a function of voltage bias.

$$\boxed{\frac{dI}{dV}(V) \propto N_B\left(E_F + eV\right)}$$

energy scale defined
by voltage bias

The zero-temperature differential conductance measures the LDOS.

Assumptions: tip DOS, constant M(E) for states involved.

If N_B = Cste, dI/dV = Cste, Ohm’s law recovered (valid also at T > 0).

The tunneling spectroscopy, general case

T > 0

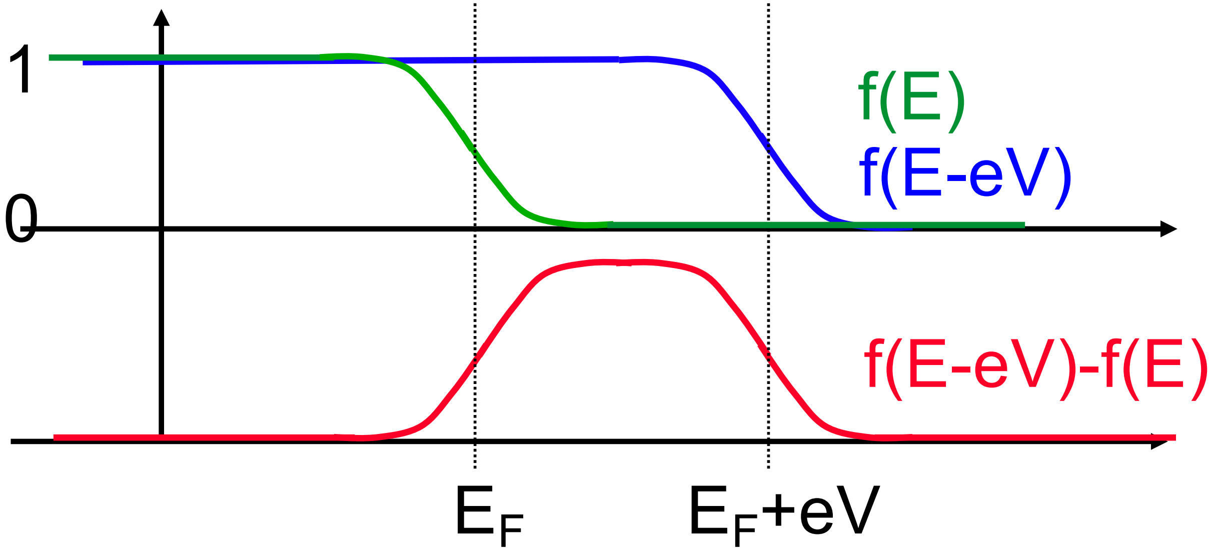

$$\boxed{\frac{dI}{dV} \propto \int_{-\infty}^{+\infty} N_B(E)\frac{d}{dV}\left(f(E-eV)\right)dE \propto \int_{-\infty}^{+\infty} \frac{e}{4k_BT}\cosh^{-2}\left(\frac{E-E_F-eV}{k_BT}\right)N_B(E)dE}$$

thermal equilibrium is assumed: f is the Fermi-Dirac function

The thermal smearing

$$\boxed{\frac{dI}{dV} \propto \int_{-\infty}^{+\infty} \frac{e}{4k_BT} \cosh^{-2}\left(\frac{E - E_F - eV}{k_BT}\right) N_B(E)dE}$$

Plot of $\frac{1}{T}\cosh^{-2}\left(\frac{E - eV}{k_BT}\right)$ for different temperatures

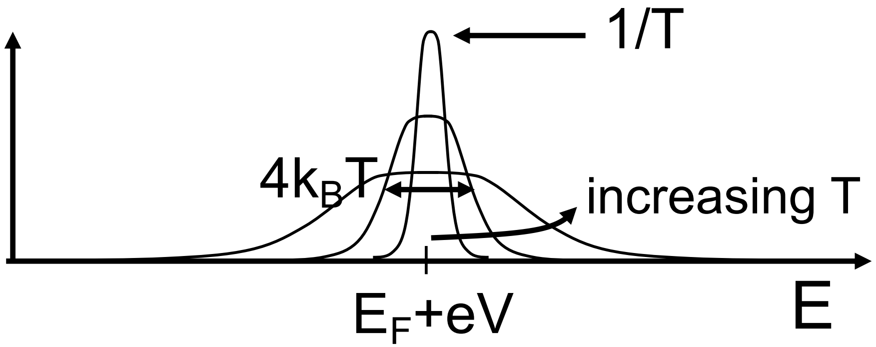

T = 0: window function is $\delta(E - eV)$, one recovers $dI/dV(V) = N_B(E_F+eV)$.

T > 0: thermal window of half-width $2k_BT$.

The diff. cond. dI/dV gives the LDOS $N_B(E)$ smeared by temperature.

Tunneling spectroscopy resolution = $2\ k_BT$: 1 K gives 0.17 meV.

Elements of superconductivity

A superconductor below T_c: zero resistance, perfect diamagnetism (B=0)

Condensation of electrons into Cooper pairs: modified DOS at the FL

BCS (from Bardeen-Cooper-Schrieffer) theory, the DOS writes:

$$N_S(E) = 0 \quad \text{if} \left|E - E_F\right| < \Delta$$

$$N_S(E) = N_N \frac{|E|}{\sqrt{(E - E_F)^2 - \Delta^2}} \quad \text{if} \left|E - E_F\right| > \Delta$$

The energy gap is :

$\Delta(T=0) = 1.76 k_B T_c$

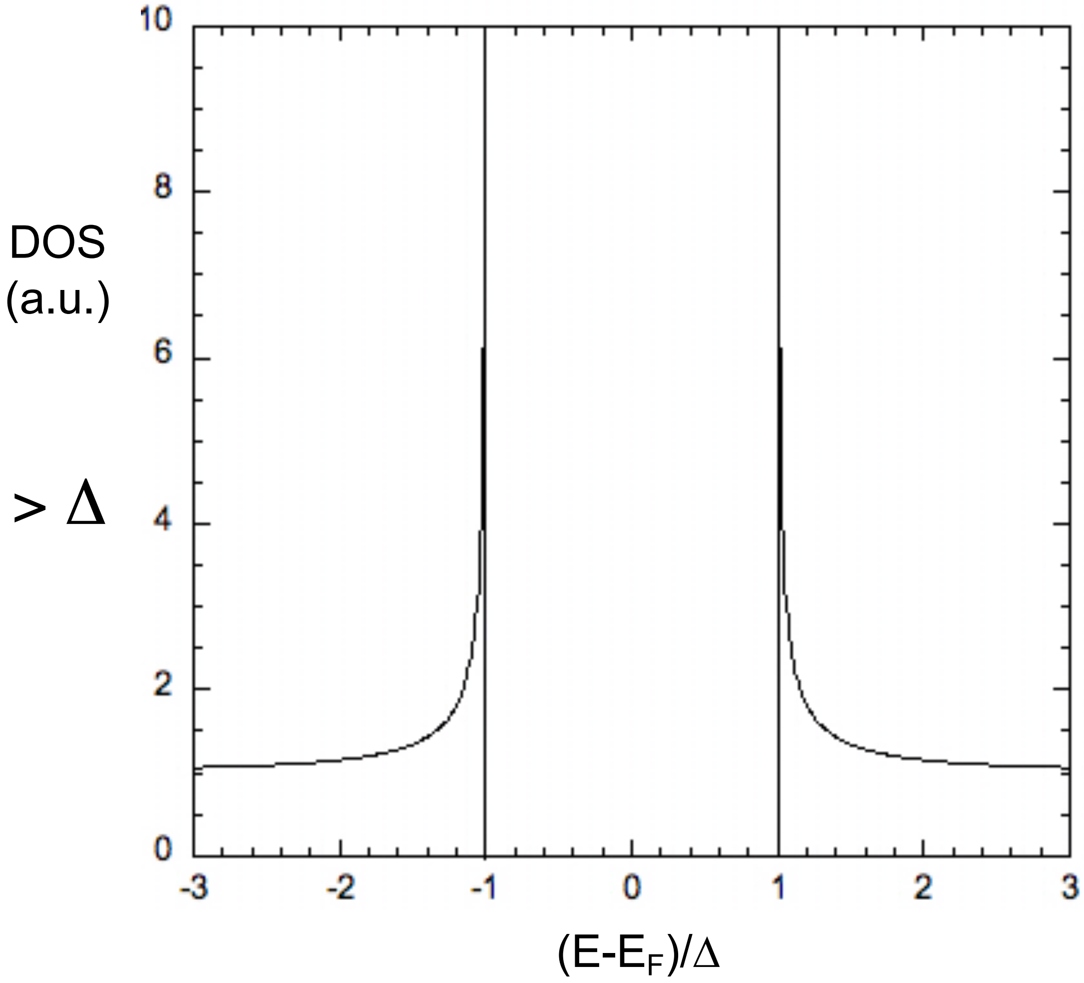

Thermal smearing of a LDOS

Example:
BCS DOS +
smearing

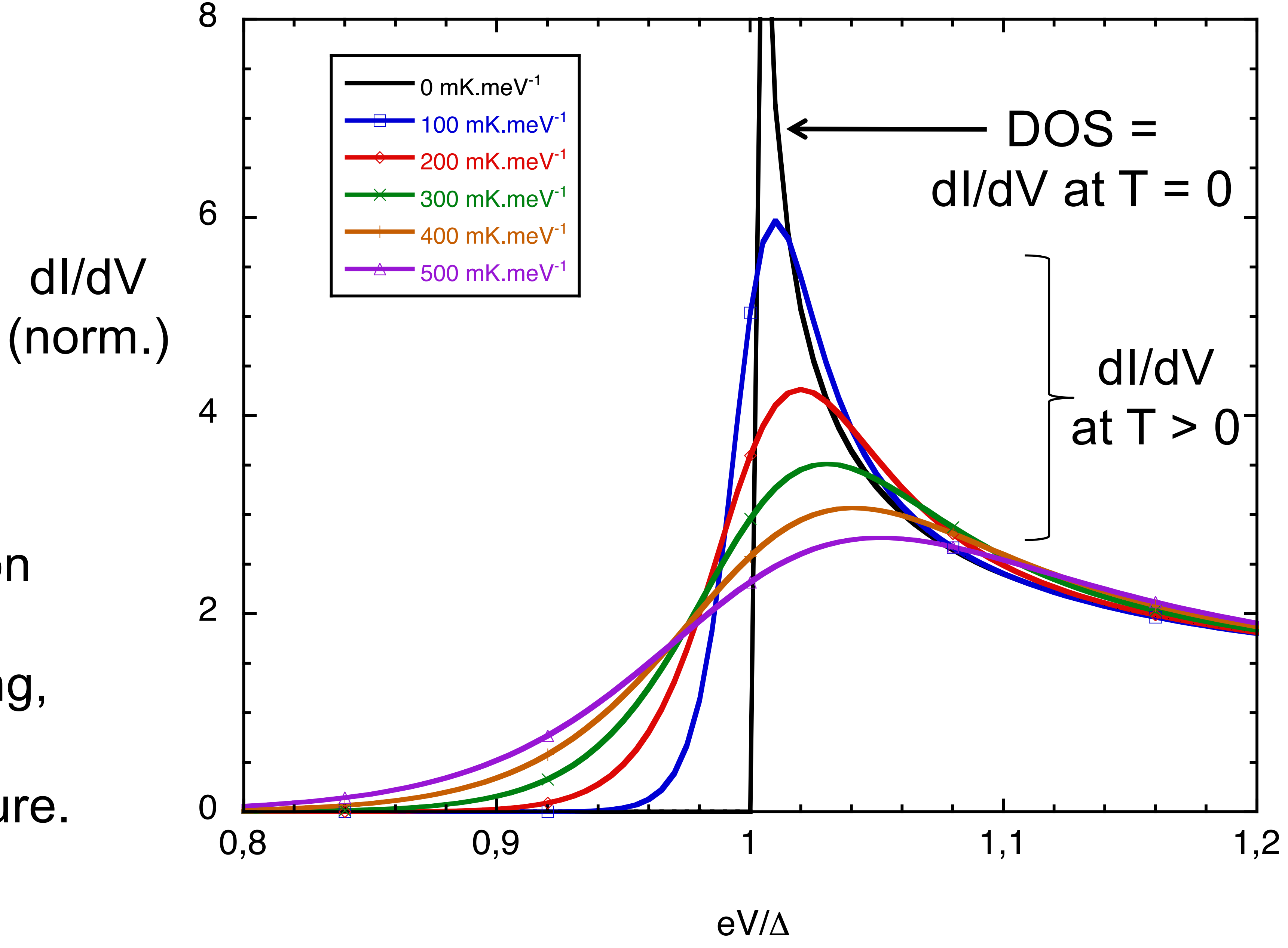

High resolution
means
small smearing,
implies
low temperature.

Chapter 1

Tunneling phenomena: from the planar junctions to the STM

1.6: History of electron tunneling

Tunneling before the STM (1)

Tunneling in planar, solid-state junctions: straightforward stability.

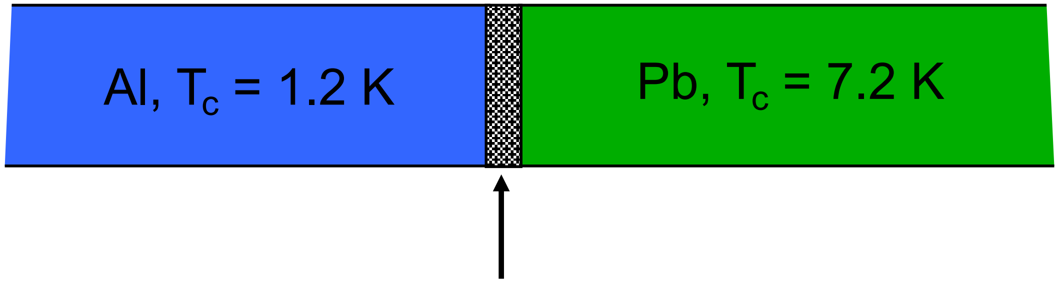

Al_2O_3 insulating barrier (a few nm):
equivalent to vacuum tunneling.

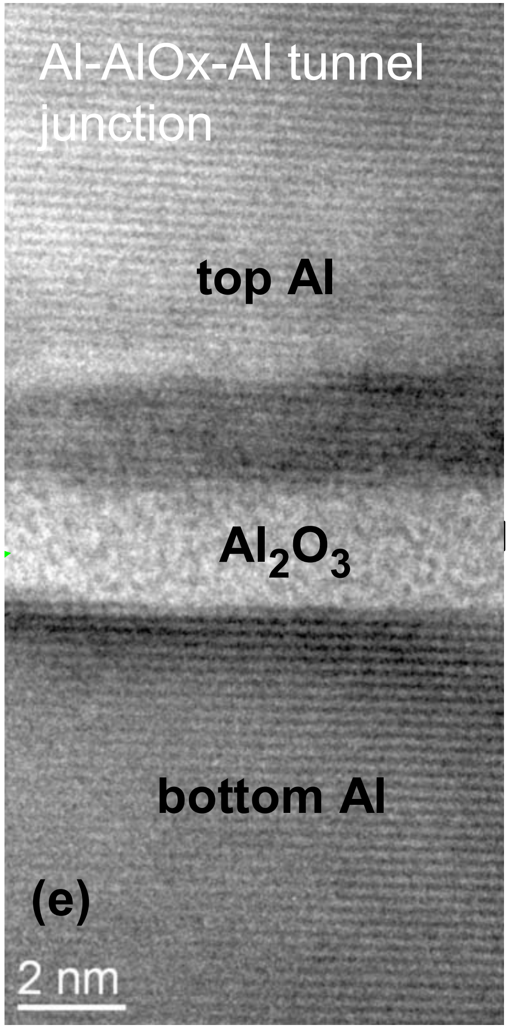

I. Giaever, Phys. Rev. Lett. 5, 147 (1960). Nobel prize 1973.
M. Prunnila et l, J. Vac. Sci. Technol. B 28, 5 (2010).

Tunneling before the STM (2)

I. Giaever, Phys. Rev. Lett. 5, 147 (1960).

Temperature regime where Pb is superconducting, Al normal.

First direct measurement of a superconducting DOS.

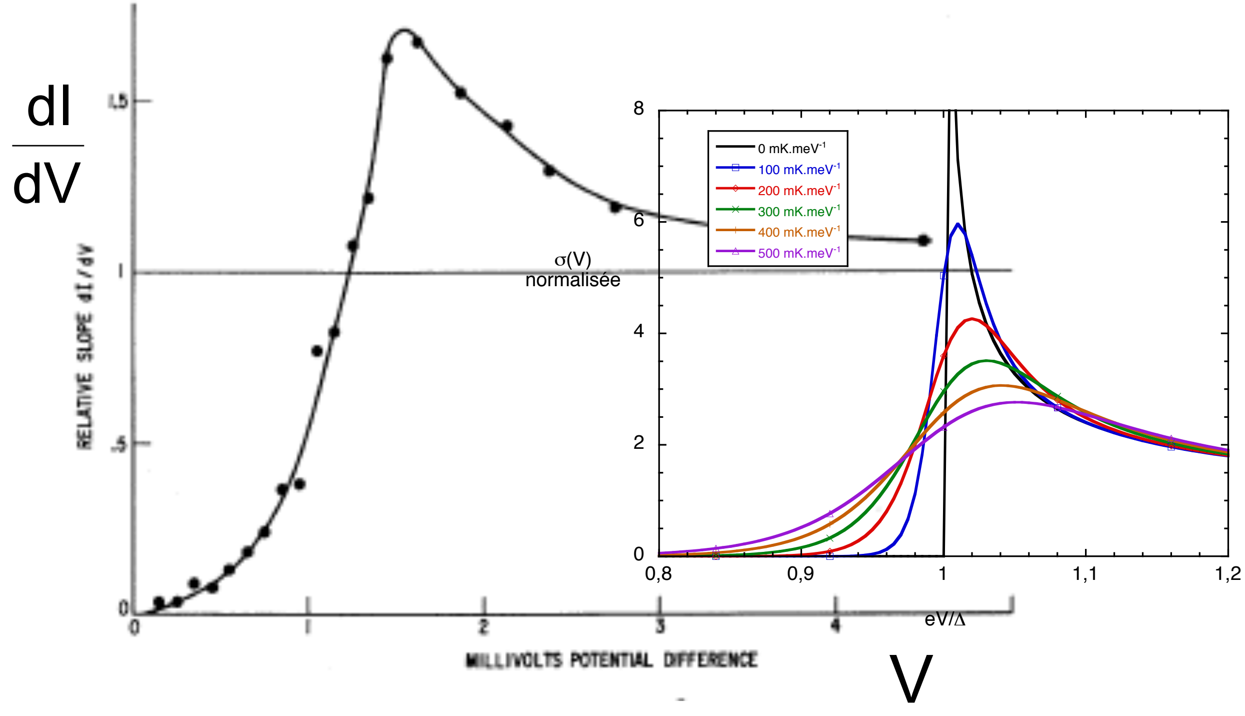

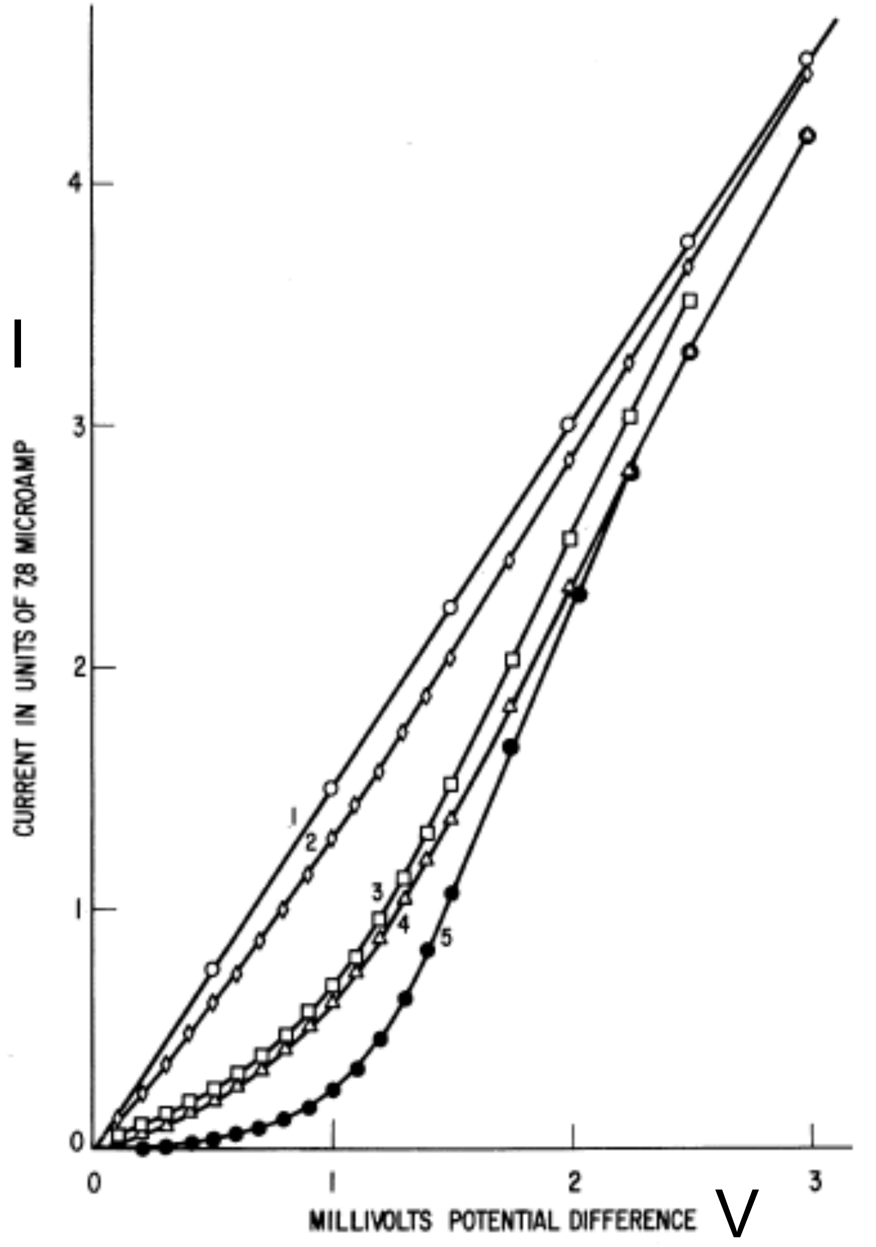

FIG. 1. Tunnel current between Al and Pb through Al$_2$O$_3$ film as a function of voltage. (1) $T=4.2$°K and 1.6°K, $H=2.7$ koe (Pb normal). (2) $T=4.2$°K, $H=0.8$ koe. (3) $T=1.6$°K, $H=0.8$ koe. (4) $T=4.2$°K, $H=0$ (Pb superconducting). (5) $T=1.6$°K, $H=0$ (Pb superconducting).

Chapter 1
Tunneling phenomena: from the planar junctions to the STM

1.7: The field emission regime

Field emission (1)

A sharp tip biased with a negative voltage :
What is the electric field at the tip apex ?

$$\boxed{E_{el} \approx \frac{V}{r}}$$

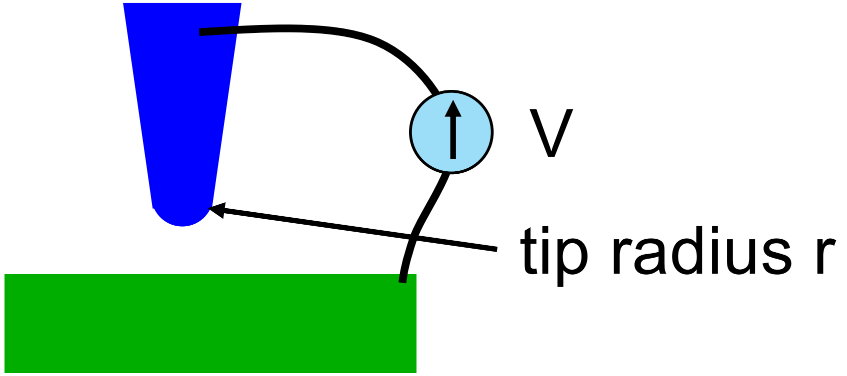

1 Volt and 10 nm give 10^{10} V/m = 1 V/Å
>> ionization field in air (3.10^6 V/m)

Huge electric fields :
unusual physics at the tip apex like atom migration.

Field emission (2)

Metallic tip at a negative potential, electric field constant at z<r:

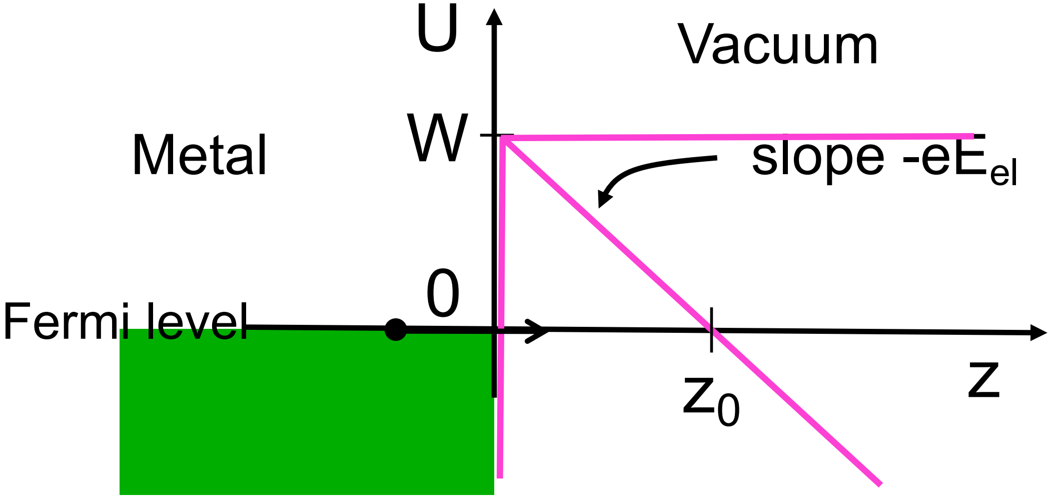

$$U(z) = W - eE_{el}z$$

$$U(z_0) = 0 \Rightarrow z_0 = \frac{W}{eE_{el}}$$

Tunneling through an electric field-induced barrier: no sample needed !

Result using WKB semiclassical approximation:

$$\boxed{T_{FE} \propto \exp\left(-\frac{4\sqrt{2m}}{3e\hbar}\frac{W^{3/2}}{E_{el}}\right)}$$

Used in Field Emission Gun in SEMs: smaller beam size, long tip life.

Transmission probabilities in practical units

W in eV
E_{el} in V/Å
d in Å

These quantities are of order 1 to 10.

Vacuum tunneling between two metals: $T_{VT} \propto \exp\left(-1.02 W^{1/2} d\right)$

Field emission: $T_{FE} \propto \exp\left(-0.68 \frac{W^{3/2}}{E_{el}}\right)$

Transmission coefficients are then of order 10^{-1} to 10^{-10}.

No distance dependence for T_{FE}: transmission depends on bias.

No field dependence for T_{VT}: Ohmic behavior expected.

Field emission versus vacuum tunneling

Between a tip and a sample at different distances:

At large distance, field emission dominates. Appears only at high voltage when el. field is large: non-linear behaviour.

At short distance, usual tunnel current dominates, ohmic behaviour (good metals).

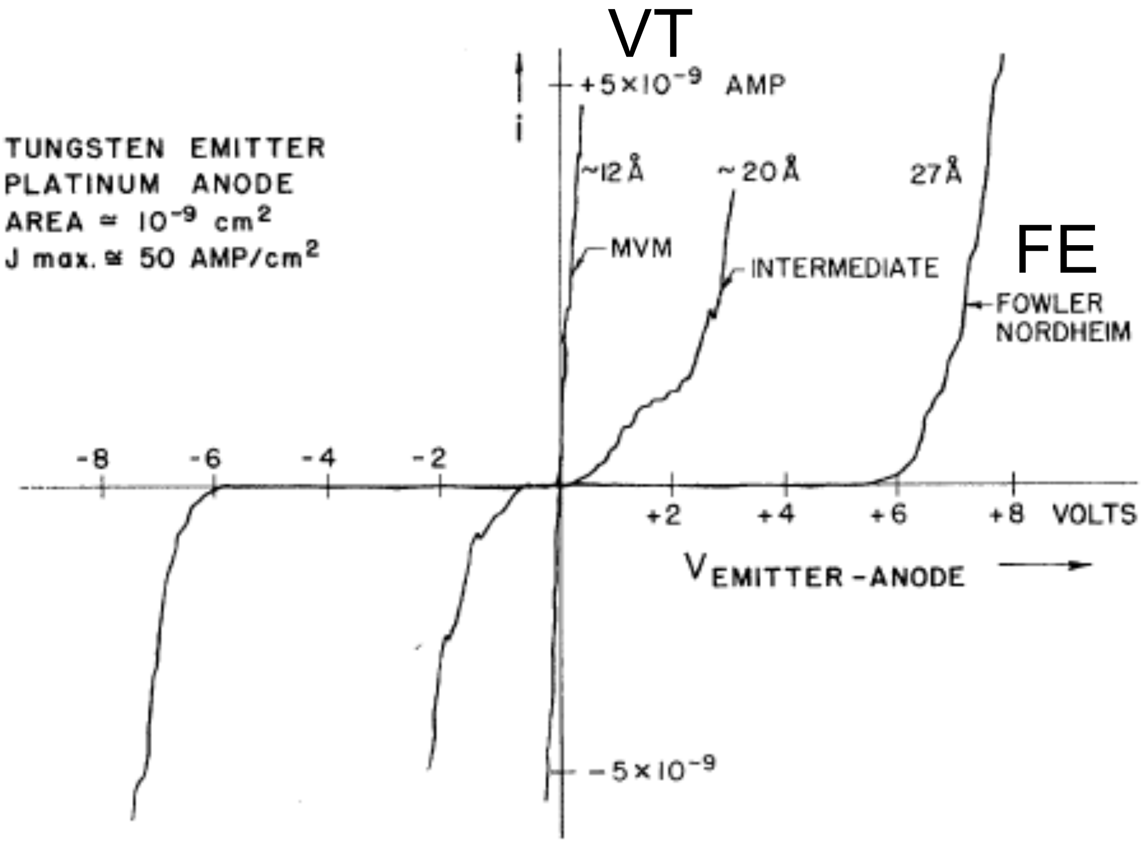

FIG. 3. Tunneling current versus voltage characteristic for three different emitter-to-surface spacings. Note the linear MVM characteristic.

R. Young et al., Phys. Rev. Lett. 27, 922 (1971)

The first scanning probe microscope ever

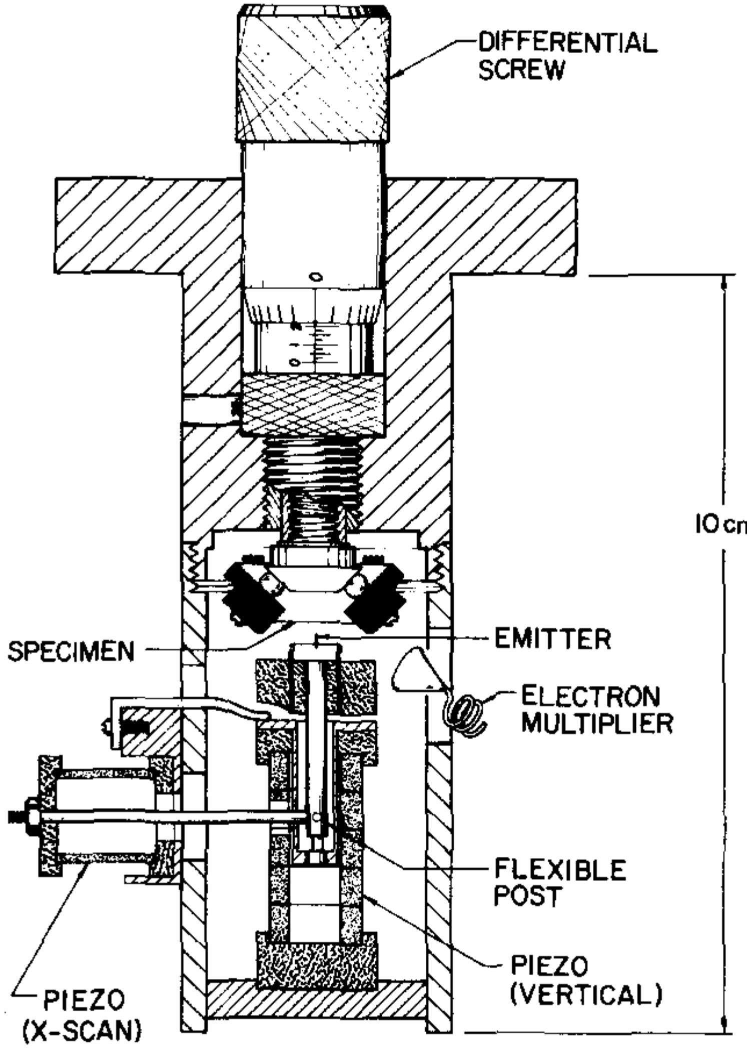

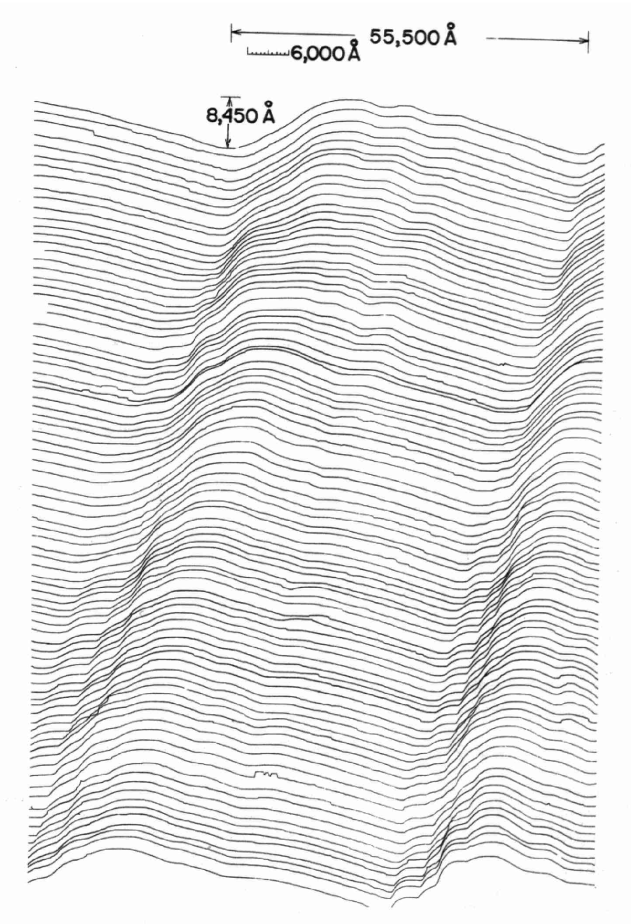

Image of a Au grating: resolution not better than an optical image.

The “topografiner“: the first scanning probe microscope.

R. Young et al., Phys. Rev. Lett. 27, 922 (1971)

Chapter 1
Tunneling phenomena: from the planar junctions to the STM

1.8: The invention of STM

The invention of STM (1)

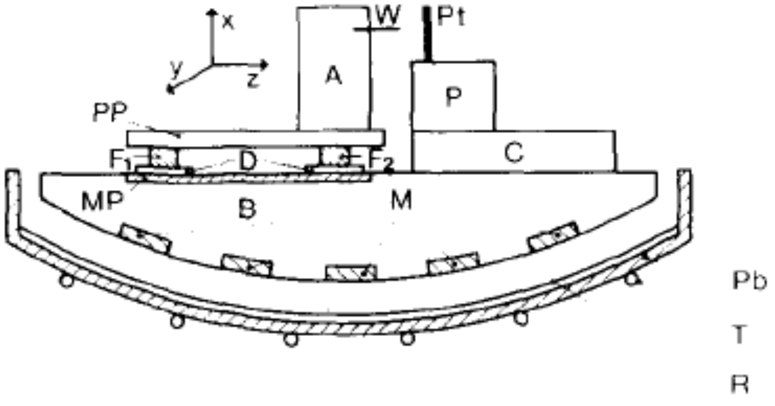

FIG. 1. Schematic of the tunneling unit and magnetic levitation system. Components and operation are described in the text. Liquid-He circulating in the tubes T cools the lead bowl Pb, which is thermally shielded by Al-coated mylar foils (not shown).

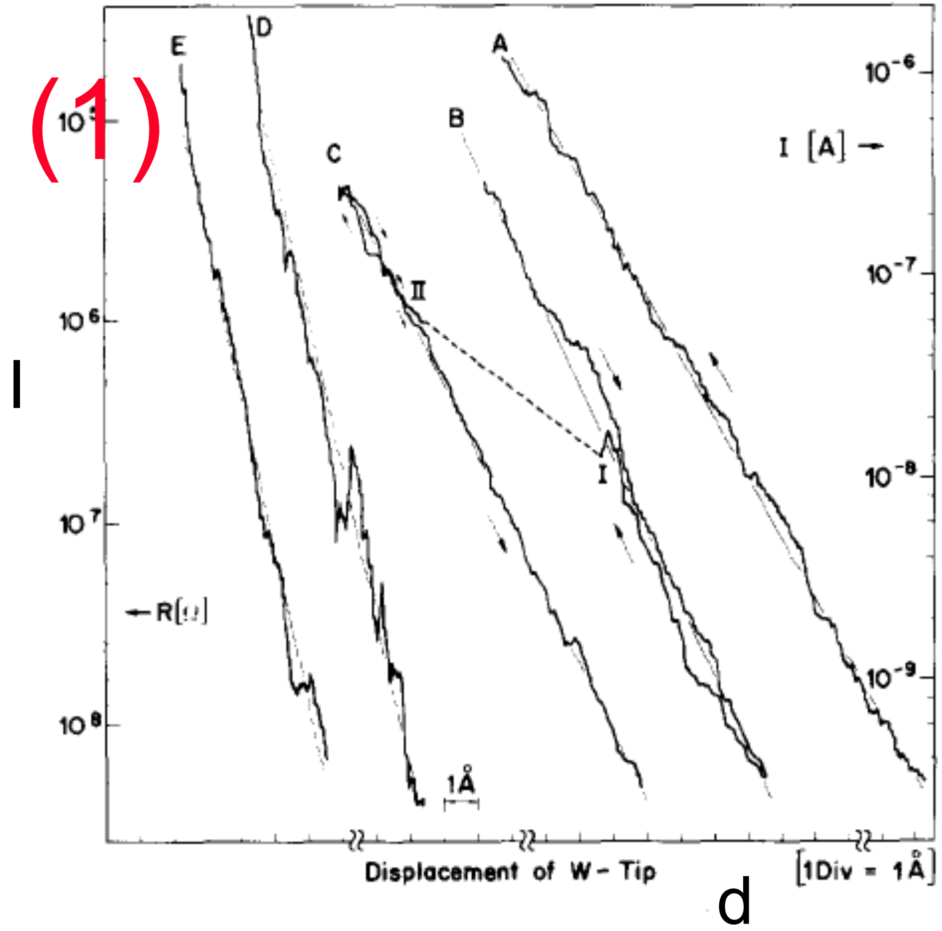

FIG. 2. Tunnel resistance and current vs displacement of Pt plate for different surface conditions as described in the text. The displacement origin is arbitrary for each curve (except for curves B and C with the same origin). The sweep rate was approximately 1 Å/s. Work functions $\phi = 0.6$ eV and 0.7 eV are derived from curves A, B, and C, respectively. The instability which occurred while scanning B and resulted in a jump from point I to II is attributed to the release of thermal stress in the unit. After this, the tunnel unit remained stable within 0.2 Å as shown by curve C. After repeated cleaning and in slightly better vacuum, the steepness of curves D and E resulted in $\phi = 3.2$ eV.

Demonstration of vacuum tunneling.

The apparent work-function depends on the tip condition (contamination).

"Tunneling through a controllable vacuum gap", G. Binnig, H. Röhrer, Ch. Gerber and E. Weibel, Appl. Phys. Lett. 40, 178 (1982).

Fig. 2: Close-up of the first scanning tunneling microscope built in 1981. (courtesy of IBM Zurich Research Laboratory)

http://www.imaging-git.com/science/scanning-probe-microscopy/microscope-design-bottom-approach

The invention of STM (2)

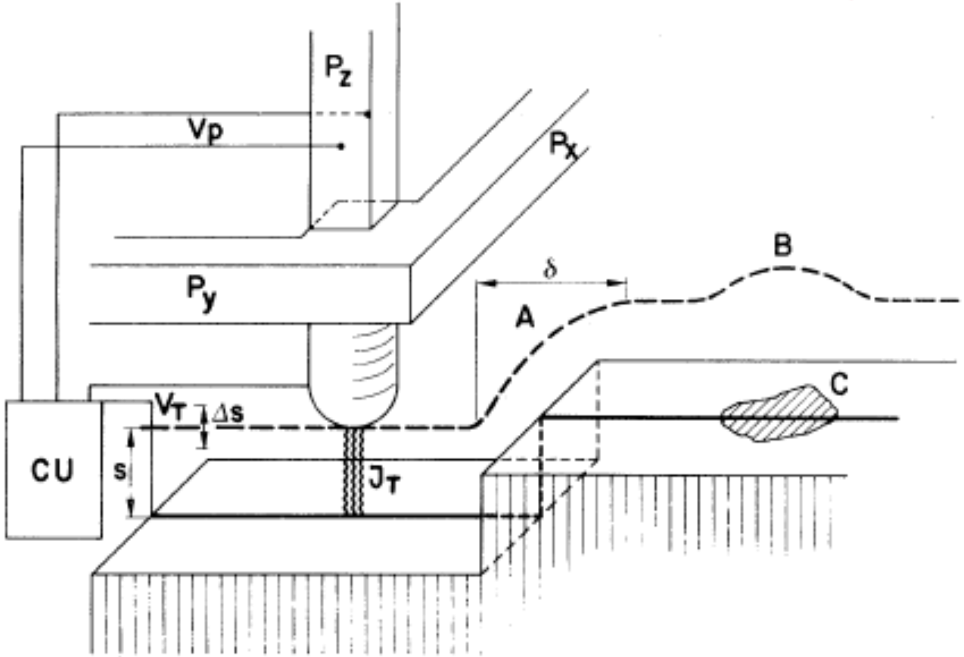

FIG. 1. Principle of operation of the scanning tunneling microscope. (Schematic: distances and sizes are not to scale.) The piezodrives P_x and P_y scan the metal tip M over the surface. The control unit (CU) applies the appropriate voltage V_p to the piezodrive P_z for constant tunnel current J_T at constant tunnel voltage V_T. For constant work function, the voltages applied to the piezodrives P_x, P_y, and P_z yield the topography of the surface directly, whereas modulation of the tunnel distance s by Δs gives a measure of the work function as explained in the text. The broken line indicates the z displacement in a y scan at (A) a surface step and (B) a contamination spot, C, with lower work function.

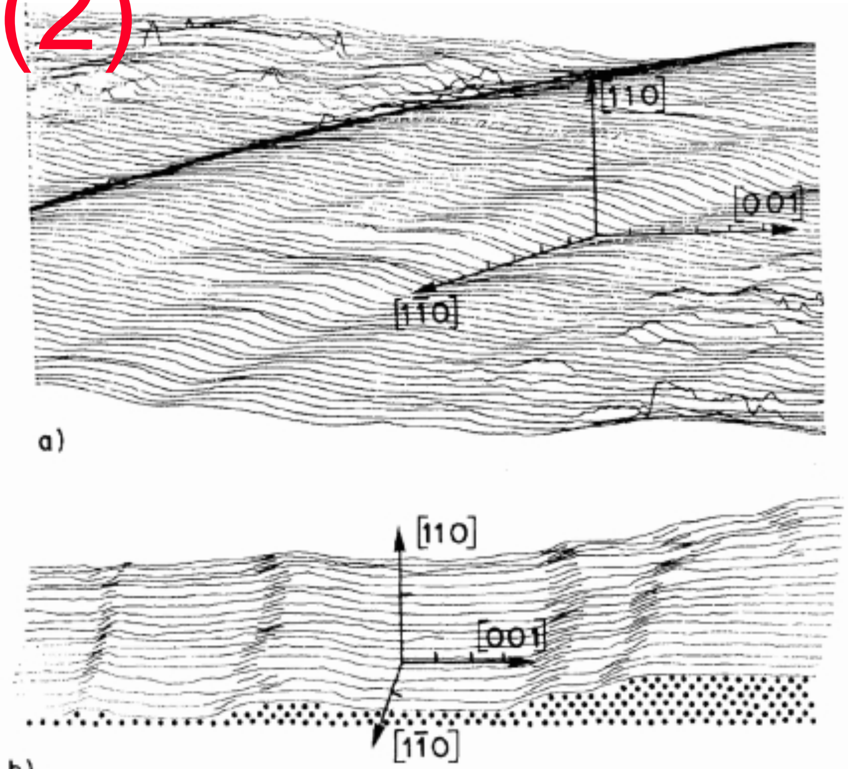

FIG. 3. Two examples of scanning tunneling micrographs of a Au (110) surface, taken at (a) room temperature, and (b) 300°C after annealing for 20 h at the same temperature (and essentially constant work function). The sensitivity is 10 Å/div everywhere. Because of a small thermal drift, there is some uncertainty in the crystal directions in the surface. In (a), the surface is gently corrugated in the [001] direction, except for a step of four atomic layers (≅ 2 atomic radii) along the [1$\bar{1}$0] direction, as indicated by the discontinuity of the shaded ribbon. The steps in (b), which were always found along the [1$\bar{1}$0] direction, are visualized by the possible positions of the Au atoms (dots).

“Surface studies by scanning tunneling microscopy” , G. Binnig, H. Röhrer, Ch. Gerber and E. Weibel, Phys. Rev. Lett. 49, 57 (1982).

The Si (111) reconstruction

Si (111) annealed at 1000° C, slow cooling-down.

First atomic-resolution image.

STM gave the exact nature of the surface left unknown by LEED exp.

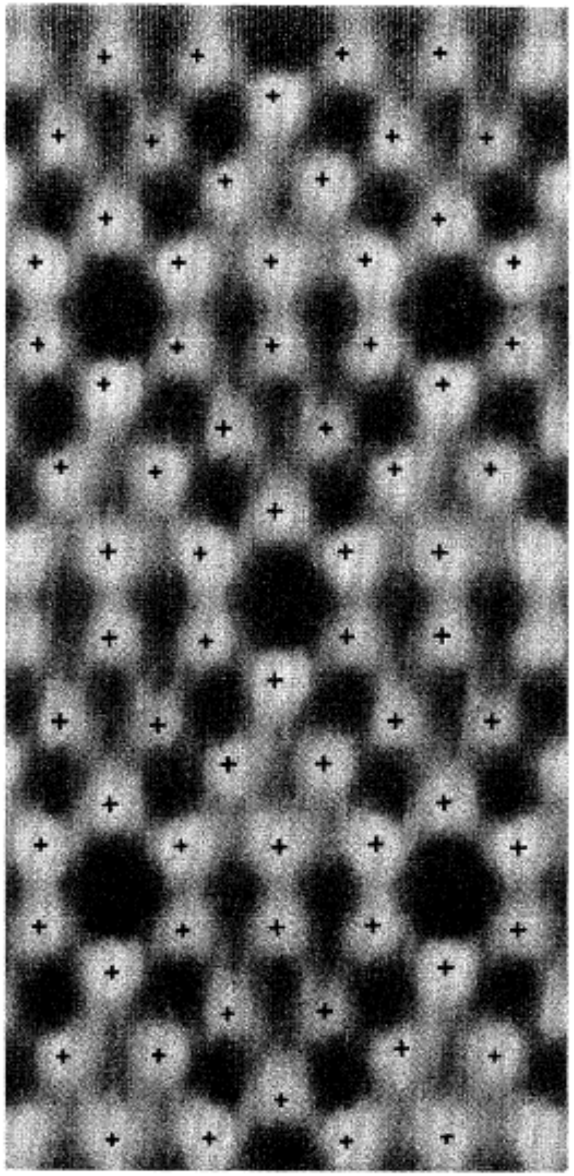

FIG. 2. Top view of the relief shown in Fig. 1 (the hill at the right is not included) clearly exhibiting the sixfold rotational symmetry of the maxima around the rhombohedron corners. Brightness is a measure of the altitude, but is not to scale. The crosses indicate adatom positions of the modified adatom model (see Fig. 3) or "milk-stool" positions (Ref. 5).

Si (111) 7x7: the model

In the bulk: diamond-like structure.

7x7 reconstruction minimizes nb of pending bonds : 49->19

Miller index refer to the number (= 7) of atomic cells involved.

In STM, the adatoms only are visible, a well as the corner vacancies.

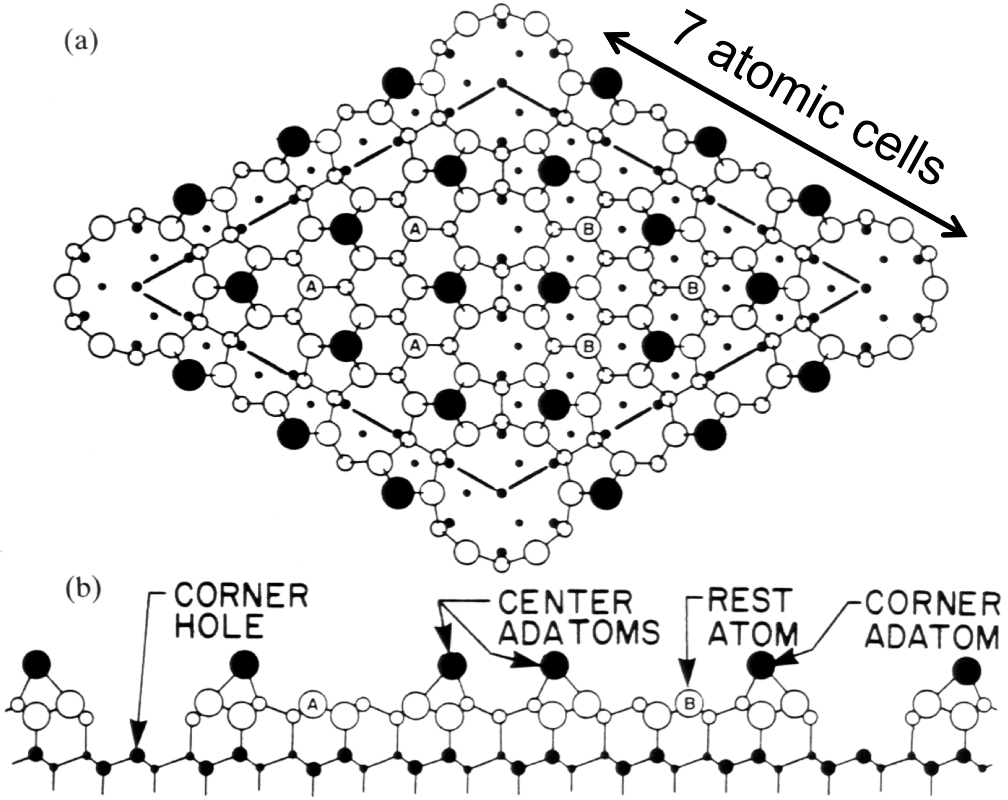

Fig. 4.2. DAS model of the Si(111) (7×7) surface. (*a*) Top view. Atoms o (111) layers at decreasing heights are indicated by circles of decreasing size Heavily outlined circles represent 12 adatoms. Larger open circles represen atoms in the stacking fault layer. Smaller open circles represent atoms in th dimer layer. Solid circles and dots represent atoms in the unreconstructed laye beneath the reconstructed surface. (*b*) Side view. Larger open and solid circle indicate atoms on the ($\bar{1}01$) plane parallel to the long diagonal across the corne vacancies of the (7×7) unit cell. Smaller open and solid circles indicate atom on the next ($\bar{1}01$) plane (Takayanagi *et al.*, 1985b).

Hard-paper work from trace-recorder data.

“7x7 reconstruction on Si (111) resolved in real space”, G. Binnig, H. Röhrer, Ch. Gerber and E. Weibel, Phys. Rev. Lett. 50, 120 (1983).

Nobel prize 1987.

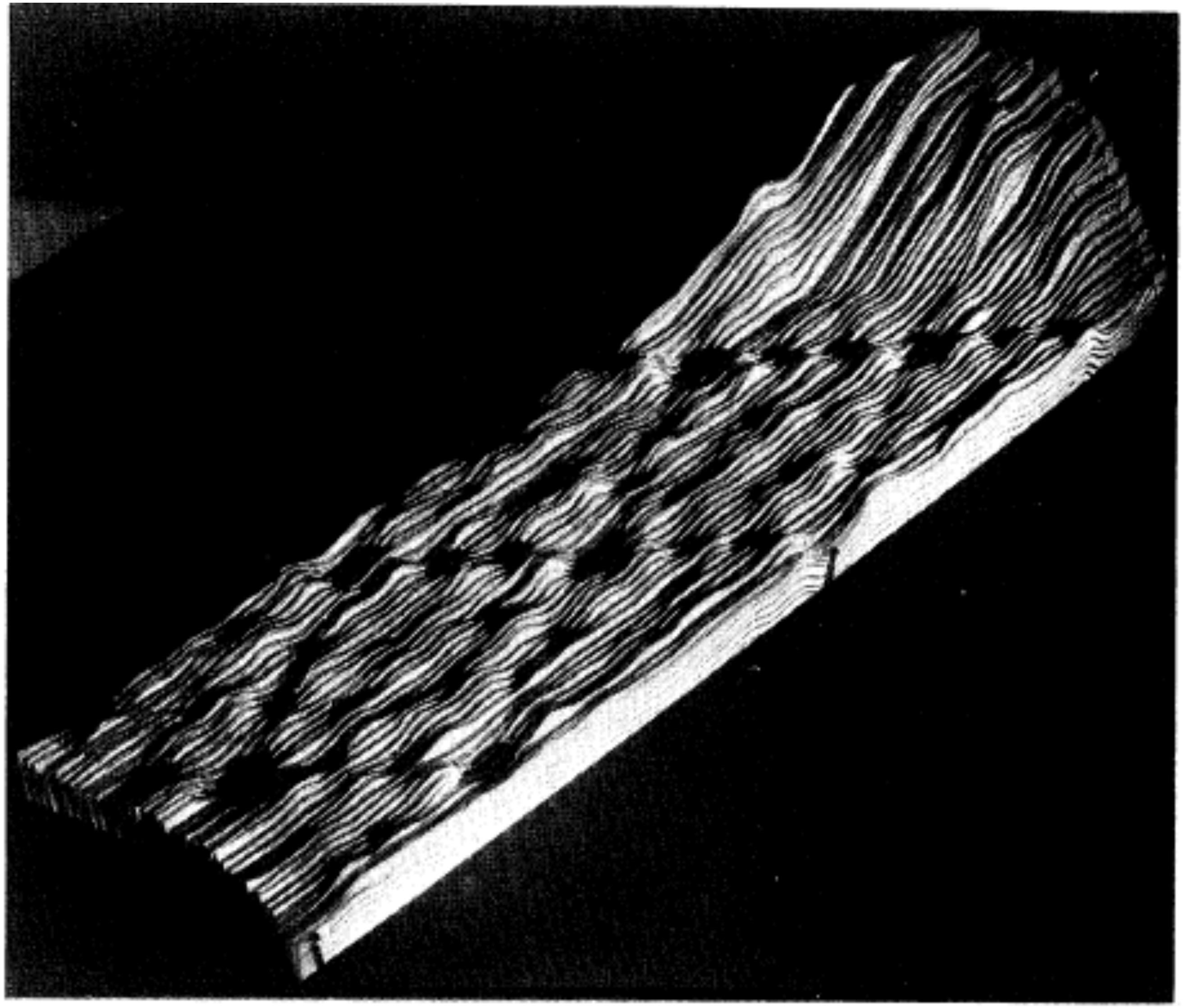

FIG. 1. Relief of two complete 7× 7 unit cells, with nine minima and twelve maxima each, taken at 300 °C. Heights are enhanced by 55%; the hill at the right grows to a maximal height of 15 Å. The $[\bar{2}11]$ direction points from right to left, along the long diagonal.

Si (111) 7x7

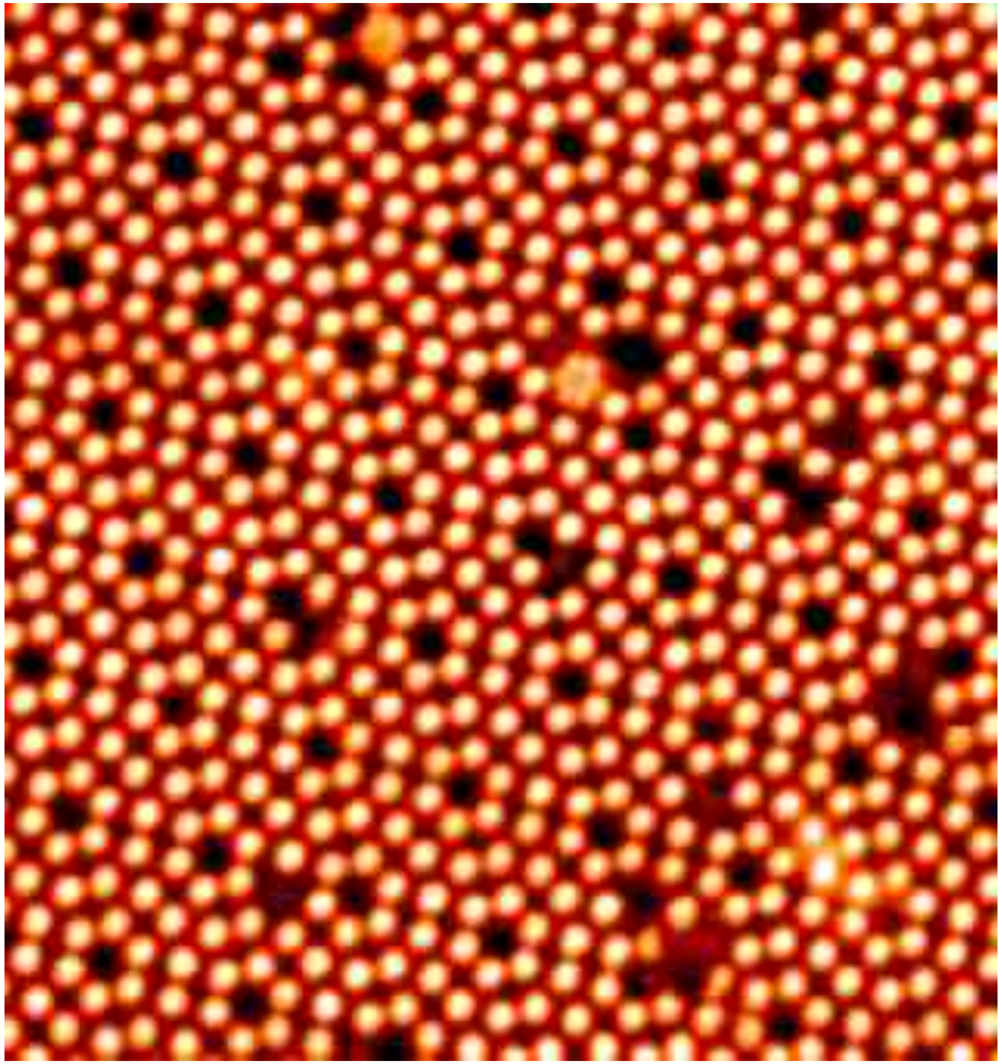

True atomic resolution.

Single vacancies and single ad-atoms visible.

Omicron website